

Identification and Counting White Blood Cell Subtypes with Convolutional Neural  
Network



A Thesis Submitted in Partial Fulfillment of the Requirements  
for the Degree of Master of Engineering in Electrical Engineering

Department of Electrical Engineering

FACULTY OF ENGINEERING

Chulalongkorn University

Academic Year 2021

Copyright of Chulalongkorn University

การระบุและนับชนิดย่อยเซลล์เม็ดเลือดขาวด้วยโครมซายประสาทเชิงสังวัตนาการ



วิทยานิพนธ์นี้เป็นส่วนหนึ่งของการศึกษาตามหลักสูตรปริญญาวิศวกรรมศาสตรมหาบัณฑิต  
สาขาวิชาวิศวกรรมไฟฟ้า ภาควิชาวิศวกรรมไฟฟ้า  
คณะวิศวกรรมศาสตร์ จุฬาลงกรณ์มหาวิทยาลัย  
ปีการศึกษา 2564  
ลิขสิทธิ์ของจุฬาลงกรณ์มหาวิทยาลัย

Thesis Title Identification and Counting White Blood Cell Subtypes  
with Convolutional Neural Network

By Mr. Singgih Bekti Worsito

Field of Study Electrical Engineering

Thesis Advisor Assistant Professor SUREE PUMRIN, Ph.D.

---

Accepted by the FACULTY OF ENGINEERING, Chulalongkorn University in  
Partial Fulfillment of the Requirement for the Master of Engineering

THESIS COMMITTEE

..... Dean of the FACULTY OF  
ENGINEERING  
(Professor SUPOT TEACHAVORASINSKUN, D.Eng.)

..... Chairman  
(Professor Doctor PONLAPAT ROJNUCKARIN)

..... Thesis Advisor  
(Assistant Professor SUREE PUMRIN, Ph.D.)

..... Examiner  
(Associate Professor WANCHALERM PORA, Ph.D.)

..... External Examiner  
(Professor Doctor Sanya Mitaim)

ชิ่งกี เบคตี เวอซีโต :

การระบุและนับชนิดย่อยเซลล์เม็ดเลือดขาวด้วยโครงข่ายประสาทเชิงสังวัตนาการ. ( Identification and Counting White Blood Cell Subtypes with Convolutional Neural Network) อ.ที่ปรึกษาหลัก : ผศ. ดร.สุรียีย์ พุ่มรินทร์

เซลล์เม็ดเลือดขาวแบ่งออกเป็น 5 ชนิดย่อย คือ นิวโทรฟิล (Neutrophil) อีโอซิโนฟิล (Eosinophil) เบโซฟิล (Basophil) ลิมโฟไซต์ (Lymphocyte) และโมโนไซต์ (Monocyte) ซึ่งเซลล์เม็ดเลือดขาว จัดเป็น ส่วนสำคัญ ในการสร้าง ระบบ ภูมิคุ้มกัน และต่อต้าน เชื้อโรค ที่เข้าสู่ร่างกาย มีการประยุกต์ ใช้ แบบจำลอง การตรวจจับวัตถุ ผ่านกล้องจุลทรรศน์ เพื่อช่วยผู้เชี่ยวชาญ ในการปฏิบัติงาน การวิเคราะห์เลือด เนื่องจาก องค์ประกอบเซลล์ ที่ไม่สมดุล ของชนิดย่อย เซลล์เม็ดเลือดขาว จึงเป็นความท้าทาย ต่อการตรวจจับเซลล์ ด้วยการ สร้างแบบจำลอง โครงข่ายประสาท เชิงสังวัตนาการ (Convolutional Neural Network: CNN) งานวิจัยนี้ มีวัตถุประสงค์ เพื่อรู้จำ และนับชนิดย่อย เซลล์เม็ดเลือดขาว ด้วยโครงข่าย ประสาท ที่สร้าง จากการ เพิ่มปริมาณ ข้อมูล (Data Augmentation) โดยโครงข่าย ประสาท เชิงสังวัตนาการ ที่นำมาประยุกต์ ใช้ในการศึกษานี้ ได้แก่ แบบจำลองแบบ YOLOv5s YOLOv5l และ YOLOv5x ในการตรวจจับ และนับ ชนิดย่อย เซลล์เม็ดเลือดขาว ซึ่งในงานวิจัยนี้ มีการเตรียมข้อมูลทั้งหมด 3 ประเภท ได้แก่ ชุดข้อมูล ที่หนึ่ง เป็นข้อมูลดิบ ที่มีจำนวนจำกัด และไม่สมดุล ชุดข้อมูลที่สอง เป็นการเพิ่มปริมาณ ข้อมูลด้วยวิธี ทางเรขาคณิต และชุดข้อมูลที่สาม เป็นการ เพิ่มปริมาณข้อมูล ด้วยการปรับปรุงภาพ จาก ผลการทดลองพบว่า แบบจำลอง ที่ให้ความแม่นยำ มากที่สุด สำหรับระบบ การรู้จำ และการนับ สำหรับ เซลล์เม็ดเลือดขาว 5 ชนิดย่อย คือ แบบจำลอง YOLOv5l โดยการนำ แบบจำลอง YOLOv5l มาประยุกต์ ใช้กับชุดข้อมูล ที่มีการเพิ่มปริมาณ ข้อมูล ด้วยการ ปรับปรุงภาพ จะให้ค่าความแม่นยำ มากที่สุด โดยมี ค่าความแม่นยำ เฉลี่ย (Mean Average Precision : mAP) ที่ mAP@.5 เท่ากับ 0.995 และ ที่ mAP@.5:.95 เท่ากับ 0.988 สำหรับ การทำซ้ำทั้งหมด 600 รอบ

สาขาวิชา วิศวกรรมไฟฟ้า

ลายมือชื่อนิสิต .....

ปีการศึกษา 2564

ลายมือชื่อ อ.ที่ปรึกษาหลัก .....

# # 6370394221 : MAJOR ELECTRICAL ENGINEERING

KEYWORD: convolutional neural network (CNN), YOLOv5, White Blood Cells,  
Subtypes, Image augmentation

Singgih Bekt Worsito : Identification and Counting White Blood Cell  
Subtypes with Convolutional Neural Network. Advisor: Asst. Prof. SUREE  
PUMRIN, Ph.D.

White blood cell (WBC) has five subtypes namely neutrophil, eosinophil, basophil, lymphocyte, and monocyte which play specific roles in the immune system and against diseases. The object detection model applied to microscopic objects is introduced to assist experts in performing tasks in blood analysis. Unbalanced cell composition of WBC subtypes to be detected is a challenge in building a model in Convolutional Neural Network (CNN). This research aims to build models in recognizing and counting WBC subtypes with neural networks constructed from augmented data enrichment. CNN is demonstrated in this study with the YOLOv5s, YOLOv5l, and YOLOv5x models to detect and count WBC subtypes. Generating three different datasets, the first is raw data with a limited and unbalanced amount, the second dataset is augmented data with geometric operation based, and the third dataset is augmented data with image enhancement based. The experimental results show that in recognition and counting systems for the five subtypes of WBC, the best model among the three models of the YOLOv5 family is YOLOv5l. The best accuracy among built models is YOLOv5l from the augmentation with image enhancement based which has an accuracy of Mean Average Precision (mAP) mAP@.5 0.995 and 0.988 mAP@.5:.95 at 600 epochs of training.

Field of Study: Electrical Engineering

Student's Signature .....

Academic Year: 2021

Advisor's Signature .....

## ACKNOWLEDGEMENTS

This project would not have been possible without the support of many people. I would like to express my sincere gratitude to my supervisor Asst. Prof. Dr. Suree Pumrin who reads my numerous revisions and helps make some sense of the confusion and for her continuous support during the past 2 years. This thesis would have never been completed without her assistance, patience, guidance, and support.

I would also like to thank the members of the committees. Sincerely and thank you to Prof. Dr. Ponlapat Rojnuckarin as a cooperative researcher from the Division of Haematology, Department of Medicine, Faculty of Medicine, Chulalongkorn University who help, correct, and revise me in the classifying process for determining the dataset in this research. Conducting everything completely online in the simple explanation to finish this work is not as simple as I imagine, without his guidance and time this research is not possible to be finished properly. I also thank Assoc. Prof. Dr. Wanchalerm Pora, and Prof. Dr. Sanya Mitaim, for their critical reviews and advice on my thesis. Your encouraging words and thoughtful, detailed feedback have been very important to me.

I would like to thank the “ASEAN and Non-Asean Scholarship” for supporting my study fully. It will not be missed, thanks also to the Embedded System and Integrated Circuit Design Laboratory (ESID Lab) for providing me with facilities and resources perfectly for my research. Additionally, this research is conducted using “MicrosisDCN” intelligent camera for microscope from Chulalongkorn University: CU\_GI\_62\_18\_21\_03, providing a machine vision prototype for this data acquisition.

Also, I appreciate all members of the ESID lab, Mr. Natthakorn Kasamsumran, Mr. Phumiphat Charoentanawat, and every member for the discussion. They have spent their valuable time giving me suggestions and guidance, moreover to Mr. Jakkrapan Sudthipadh (P’Map) always has a fast response to the message and help me to connect to my computer when it's disconnected suddenly sometimes.

I am grateful for my friends for a good environment to shine together, and immense gratitude as always to dr. Nyan Linn, one of my good friends, a Ph.D student

from the College of Public Health Sciences for his patience and support in the discussion of this thesis during the badminton match. You help me in the discussion from the beginning to make this proposed object clear when I am asking in confusion. We know that it is important to strike a balance with life outside the dark depths of the lab with the sport for refreshing. Gratefully I would like to thank my teams in the Overseas Indonesian Students' Association Alliance (OISAA/PPID) around the world and in Thailand for having remarkable discussions and projects when we don't have enough ecosystem for study during COVID-19 periods.

Finally, and most importantly I would like to express my deepest gratitude to my family, for their constant, unconditional, unequivocal, and loving support, and affectionate encouragement during this journey.

Singgih Bektī Worsito



## TABLE OF CONTENTS

	Page
ABSTRACT (THAI).....	iii
ABSTRACT (ENGLISH).....	iv
ACKNOWLEDGEMENTS.....	v
TABLE OF CONTENTS.....	vii
List of Tables.....	x
List of Figures.....	xii
CHAPTER 1 INTRODUCTION.....	1
1.1. Background.....	1
1.2. Objective.....	3
1.3. The Scope of Research.....	3
1.4. Research Methods.....	3
1.5. Expected Benefits.....	4
CHAPTER 2 LITERATURE REVIEW.....	5
2.1. Related Works.....	5
2.2. Blood Cell.....	7
2.2.1. Complete Blood Cell.....	7
2.2.2. Subtypes of WBC.....	9
2.3. Machine Learning.....	12
2.4. Convolutional Neural Network (CNN).....	14
2.5. YOLO (You Only Look Once).....	17
CHAPTER 3 METHOD.....	23



3.1. Data Acquisition.....	23
3.2. Data Augmentation .....	24
3.3. Data Splitting.....	25
3.4. Data Annotation.....	26
3.5. Design and Implementation.....	27
3.6. Testing and Evaluation.....	27
CHAPTER 4 RESULT AND DISCUSSION .....	29
4.1. Data Collection.....	29
4.2. Image Augmentation.....	38
4.3.1. Geometric Operation-based .....	38
4.3.1. Image Enhancement-based .....	41
4.3. Training Result of Raw Data .....	45
4.3.1. YOLOv5s.....	48
4.3.2. YOLOv5l .....	50
4.3.3. YOLOv5x .....	52
4.4. Training Result of Augmented Data.....	54
4.4.1. YOLOv5s.....	56
4.4.2. YOLOv5l .....	58
4.4.3. YOLOv5x .....	60
4.4.4. YOLOv5l image enhancement-based .....	62
4.5. Comparison of Training Result.....	64
4.5.1. Geometric Operation.....	64
4.5.2. Image Enhancement .....	65
4.6. Blood Counting.....	67

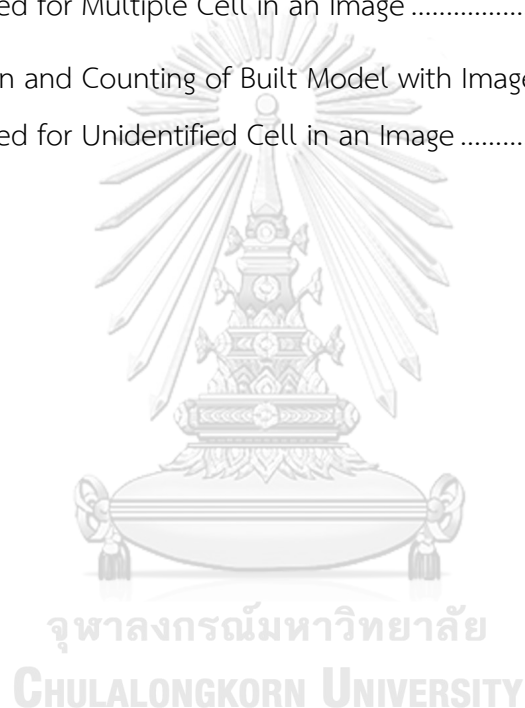
4.6.1. YOLOv5 Counting (Raw Data Model) .....	71
4.6.2. YOLOv5 Counting (Augmented Data Model).....	74
4.6.1. YOLOv5l Counting (Image Enhancement-based)) .....	77
CHAPTER 5 CONCLUSION .....	81
5.1. Conclusion .....	81
5.2. Future Work.....	81
REFERENCES .....	83
VITA.....	90



## List of Tables

	<b>Page</b>
Table 1. Blood Types.....	7
Table 2. MicrosisDCN Specification .....	30
Table Table 3. Raspberry PI OS Installation.....	31
Table 4. Data Observation .....	32
Table 5. Captured Images with Different Magnification.....	34
Table 6. Raw Data.....	37
Table 7. Augmentation through Multiplication Factor.....	39
Table 8. Distribution of Augmented Images.....	40
Table 9. An image enhancement-based augmentation dataset .....	43
Table 10. Distribution of image enhancement-based augmentation dataset .....	44
Table 11. YOLOv5 Version .....	47
Table 12. Data Splitting for Augmented Data .....	55
Table 13. Built Models from Raw Data .....	64
Table 14. Built Models from Enrichment Data through Geometric Operation .....	64
Table 15. YOLOv5l in 3 different datasets .....	66
Table 16. Detection and Counting Using Model in Single Cell in an Image.....	71
Table 17. Detection and Counting from Built Model based on the Raw Data in Multiple Cell in an Image.....	72
Table 18. Detection and Counting from Built Model based on Raw Data on Unidentified Cell in an Image.....	73
Table 19. Detection and Counting from Built Model based on Geometric Operation Augmentation-based in Single Cell in an Image .....	74

Table 20. Detection and Counting of Built Model with Geometric Operation Augmentation-based for Multiple Cell in an Image .....	76
Table 21. Detection and Counting of Built Model with Geometric Operation Augmentation-based for Multiple Cell in Multiple Cell in an Image .....	77
Table 22. Detection and Counting of Built Model with Image Enhancement Augmentation-based for Single Cell in an Image.....	77
Table 23. Detection and Counting of Built Model with Image Enhancement Augmentation-based for Multiple Cell in an Image .....	79
Table 24. Detection and Counting of Built Model with Image Enhancement Augmentation-based for Unidentified Cell in an Image .....	80



## List of Figures

	<b>Page</b>
Figure 1 Subtypes of WBC.....	10
Figure 2. MLP Dimension (left) and CNN (right) .....	14
Figure 3. An Example of CNN Architecture.....	15
<i>Figure 4. Convolution Process.....</i>	<i>16</i>
Figure 5. ReLu Activation.....	16
Figure 6. Max Pooling.....	17
Figure 7. Model YOLO.....	19
Figure 8. The YOLO object detection process.....	20
Figure 9. YOLO Detection System .....	21
Figure 10. Data Acquisition Using Microscope.....	23
Figure 11. Augmentation based on Geometric Operation .....	24
Figure 12. Augmentation based on Image Enhancement .....	25
Figure 13. Data Splitting.....	26
Figure 14. Data Annotation .....	27
Figure 15. MicrosisDCN Module.....	29
Figure 16. MicrosisDCN for Image Capturing.....	30
Figure 17 . Installation Process for Raspberry PI OS.....	31
Figure 18. Data Verification .....	35
Figure 19. First Grouping.....	36
Figure 20. Data Verification .....	36
Figure 21. Data Correction .....	37

Figure 22. Prepared Augmented Images .....	40
Figure 23 . Image enhancement-based augmentation dataset .....	45
Figure 24. PyTorch Seeting Up.....	46
Figure 25. CUDA 11.3 Installation .....	46
Figure 26. YOLOv5s accuracy (Raw Data) with distributed classes.....	48
Figure 27. The comparison of YOLOv5s accuracy (Raw Data) for among WBC subtypes .....	48
Figure 28. Confusion Matrix YOLOv5s (Raw Data) .....	49
Figure 29. YOLOv5s Prediction (Raw Data) .....	49
Figure 30. YOLOv5l accuracy (Raw Data) with distributed classes .....	50
Figure 31. The comparison of YOLOv5l accuracy (Raw Data) for among WBC subtypes .....	50
Figure 32. YOLOv5l Confusion Matrix (Raw Data).....	51
Figure 33. YOLOv5l Prediction (Raw Data).....	51
Figure 34. YOLOv5x accuracy (Raw Data) with distributed classes.....	52
Figure 35. The comparison of YOLOv5x accuracy (Raw Data) for among WBC subtypes .....	52
Figure 36. YOLOv5x Confusion Matrix (Raw Data).....	53
Figure 37. YOLOv5x6 Prediction (Raw Data).....	53
Figure 38. Auto-Labeling .....	54
Figure 39. YOLOv5s accuracy (Geometric Operation based) with distributed classes	56
Figure 40. The comparison of YOLOv5s accuracy (Geometric Operation based) for among WBC subtypes.....	56
Figure 41.YOLOv5s Confusion Matrix (Geometric Operation based).....	57
Figure 42. YOLOv5s Prediction (Geometric Operation based).....	57

Figure 43. YOLOv5l accuracy (Geometric Operation based) with distributed classes..	58
Figure 44. The comparison of YOLOv5l (Geometric Operation based) accuracy for among WBC subtypes .....	58
Figure 45. YOLOv5l Confusion Matrix (Geometric Operation based) .....	59
Figure 46. YOLOv5l Prediction (Geometric Operation based) .....	59
Figure 47. YOLOv5x accuracy (Geometric Operation based) with distributed classes .	60
Figure 48. The comparison of YOLOv5x accuracy (Geometric Operation based) for among WBC subtypes .....	60
Figure 49. YOLOv5x Confusion Matrix (Geometric Operation based).....	61
Figure 50. YOLOv5x Prediction (Geometric Operation based).....	61
Figure 51. YOLOv5l accuracy (image enhancement-based data) with distributed classes .....	62
Figure 52. The comparison of YOLOv5l (image enhancement-based data) accuracy for among WBC subtypes .....	62
Figure 53. YOLOv5l Confusion Matrix (image enhancement-based data).....	63
Figure 54. YOLOv5l Prediction (image enhancement-based data).....	63
Figure 55. YOLOv5l in 3 Different Datasets .....	66
Figure 56. Counting Process.....	67
Figure 57. Testing Single Cell in Single Image.....	68
Figure 58. Testing Multiple Cell in Single Image .....	69
Figure 59. Testing No Cell in Single Image .....	70
Figure 60. Testing Unidentified Cell .....	70
Figure 61. Counting Result of YOLOv5s Model (Raw Data).....	71
Figure 62. Chart of Counting Result of YOLOv5s (Raw Data).....	72
Figure 63. Counted Cell of YOLOv5x (Raw Data) .....	73

Figure 64. Counting Result of YOLOv5l (Geometric Operation based).....	75
Figure 65. Chart of Counting Result of YOLOv5l (Geometric Operation based).....	75
Figure 66. Counted Cell of YOLOv5x (Geometric Operation).....	76
Figure 67. Counting Result of YOLOv5l using Augmentation (Image Enhancement-based).....	78
Figure 68. Chart of Counting Result of YOLOv5s (Image Enhancement).....	78
Figure 69. Counted Cell of YOLOv5l using Image Enhancement Data.....	79





## CHAPTER 1 INTRODUCTION

### 1.1. Background

The development of medical technology today is expected to be able to work more quickly, accurately, flexibly, and limitlessly. Application-based medical technology within the scope of services in the field of health teleconsultation is developed to connect medical personnel with patients [1]. The implementation of embedded systems on a hardware connected to mobile applications on smartphones is also proposed to facilitate the patient care process to the use of communication across software and hardware [2]. Handling disease is currently a global challenge where the idea of telehealth and telemedicine services is also increasing during COVID-19 [3]. Likewise, extracting information on microscopic material detection systems is a challenge in blood identification. Research on the implementation of health services, to build a smart city in the future, in supporting the transformation of a powerful city is also proposed through the concept of cloud-computing-based blood analysis services [4]. In addition, today's demands encourage humans to be able to work together online and without limits with faster and easier data exchange speeds.

Microscopy images have tons of information which is prominent completely to be analyzed in both medical and science scope. The related research is conducted for blood cell analysis based on images as the collected microscopy data to detect abnormalities in white blood cells. During this pandemic, the volume of laboratory work increases drastically but social distancing and lockdown measures force medical labs to accelerate their digital pathology capabilities [5]. The process of blood detection is still being carried out by experts in the laboratory with very good accuracy. Experts carry out direct sample testing carefully to ensure that the results can be known accurately. As a consequence, the process is time-consuming and prone to human error.

The machine learning method developed by researchers recently is intended to help in solving various problems in both general health and specific services for a certain scope. Blood analysis is an essential indicator for many diseases. It has contagiously several parameters which are a sign for specific diseases [6]. White blood cell (WBC) detection is one of the promising areas to be researched. The classification of white blood cells plays an important part in medical diagnosis. Taking consideration to the performance, in order to reduce the risk of human error, speed up work, increase detection accuracy, enable remote work, and expand the opportunity to work in higher levels, the implementation of machine learning provides positive improvements [7].

However, WBC basically has five types of subtypes namely neutrophils, eosinophils, basophils, lymphocytes, and monocytes. They are an important part of the human body that plays a prominent role in building the immune system and fighting disease. The composition of each of them is basically not the same biologically. The balance is naturally formed to maintain the stability of the body. Nearly half of the white blood cells in the body are neutrophils, which are the first cells of the immune system to respond by attacking bacteria or viruses. Eosinophils are only about one percent of the white blood cells in the bloodstream, if the number of eosinophils is excessive, it is generally the result of an immune response to an allergen. Monocytes have the ability to recognize "danger signals" which is about 5 percent of all white blood cells. In addition to the three subtypes, there are still lymphocytes and basophils [8]. This difference in composition is one of the challenges in developing a data-based detection model using machine learning.

Thus, this research will use an augmentation technique approach to proportionally enrich the dataset on the image that will be used as input. Then, the enriched data will be used as a dataset in the model building using convolutional neural network. This research aims to figure out the accuracy of the neural network model constructed from augmented data enrichment. Finally, this research proposes

the Identification of White Blood Cell Subtypes with Neural Network built with multiple augmented image mechanisms to gain accuracy trained in CNN.

## **1.2. Objective**

1.2.1. Identify and count subtypes of WBC using Neural Network with limited data.

1.2.2. Figure out detection accuracy of the Convolutional Neural Network by performing data enrichment through augmentation techniques for identification of subtypes of WBC.

## **1.3. The Scope of Research**

1.3.1. Create an image database by capturing dataset that can be used for the training process in a convolutional neural network.

1.3.2. This study uses the same ratio between the amount of training data and test data for the models built.

1.3.3. Carry out the augmentation process as a step to enrich the data by considering the multiplication factor and variables of the augmentation technique.

1.3.4. Development is constructed by using the CNN.

1.3.5. The detection system was developed for 5 classes of subtypes of white blood cells which are eosinophil, lymphocyte, monocyte, basophil, and neutrophil.

## **1.4. Research Methods**

1.4.1. Reviewing various sources of theory and related work for white blood detection using a neural network.

1.4.2. Studying several types of models of CNN.

1.4.3. Identify the characteristics of each WBC subtypes.

1.4.4. Collecting dataset from approximately 100 blood sample slides.

1.4.4. Learn the method of data enrichment through augmentation techniques.

1.4.5. Studying the training mechanism for WBC subtype image data using GPU.

1.4.6. Comparing the accuracy generated from the models built.

1.4.7. Summarize the results and write a thesis report.

1.4.8. Publication of the thesis.

### **1.5. Expected Benefits**

1.5.1. Obtain subtypes of WBC image data set.

1.5.2. Perform data augmentation for data enrichment based on multiplication factor and divide it into training data and testing data.

1.5.3. Figure out the performance of detecting subtypes of WBC and compare it to the performance of the built models.

## CHAPTER 2 LITERATURE REVIEW

### 2.1. Related Works

The implementation of technology in the white blood cells detection is proposed in many various ways. Digital transformation to support the development of civilization in a future life and smart city cannot only depend on laborious activities. A medical service system is developed with a web display based on cloud computing in the image analysis process to speed up the service process and reduce the potential for human-error [4]. The detection process can be done together with a computer by utilizing a database with many sample images and models that have been trained. Applying a trained multi-class ensemble - based mechanism in the cloud, a smartphone-based framework for localizing WBCs inside microscopic pictures of blood smears can be used. The nucleus is firstly segmented in the suggested framework, then texture, analytical, and wavelet features are extracted. Finally, five classes are determined for the identified WBCs: neutrophil basophil, eosinophil, lymphocyte, and monocyte.

Some research focus on the implementation of an image detection system on blood samples which is used to determine blood type using basic image processing. Yamin et al. [9] proposed a blood type detection system using image processing techniques offered for use in certain areas where medical personnel are not available. The same thing was also proposed by Ravindran et al. [10] where the image processing process uses several process stages such as pre-processing techniques, thresholding, morphological operations, HSL luminance plane, and quantification. However, because the system is not built based on data, it can be disturbed in certain conditions such as light exposure and size.

There are approach focuses on the consolidation of blood detection and machine learning. Ashour et al. [11] proposed basophils and eosinophils detection with a stratified system using deduced histogram-based image processing to determine the most appropriate color field for initial WBC detection and then proceed with a classification-based segmentation process. Finally, this detection

system has perfect performance by using the support vector machine (SVM) method. Nevertheless, white blood cells have morphological variations that can complicate the segmentation process and on its accuracy.

Another study discusses the WBC detection system, where D. Wang et al. [12] use limited dataset from an institution. Due to the lack of data, this study augments the data with a reflection operation with the initial data and the augmented data being 609 and 1218 images, respectively. In the training process into the neural network, the study uses a ratio of 90% data for training and 10% data for testing. The model is developed using an improved Faster-RCNN model to classify the white blood cells in the dataset and got magnificent accuracy. However, the study does not discuss in detail the geometric operations used in augmentation.

CNN in biomedical field is proposed by Igarasiha et al. [13] to classify the anatomy of the upper gastrointestinal organs using AlexNet under various picture collection circumstances. Kardy et al. [14] suggests studying the automatic leukocyte segmentation from hematological pictures using several CNN algorithms where CNN is a resource for medical analysis. The study separates the leukocyte segment from the hematological images that have been RGB scaled. U-Net, and VGG-UNet are only a few of the CNN-based segmentation techniques used in the proposed study. The Leukocyte Images for Segmentation and Classification (LISC) database provided the images that we utilized. However, the study does not produce the dataset through image acquisition and just focuses on leucocyte in general.

Another study performs image enrichment by rotating the initial images. Sharif et al. [15] propose the recognition in distinguishing subtypes of WBC using YOLOv2 model with the augmented images from the initial to augmented images is 250 and 6250 respectively. The augmentation is performed by implementing the scaling and rotation at 30°, 45°, 90°, 180°, 240°, and 360° to increase the number of total data to 6250 images. That study is perfectly done by showing magnificent accuracy and evaluation. But it does not perform other augmentation techniques based on the geometric operation.

## 2.2. Blood Cell

### 2.2.1. Complete Blood Cell

Blood is composed from the amount of blood plasma and blood cells, all of which circulate throughout the body. These blood cells are further divided into three types, namely red blood cells, white blood cells, and platelets. All of its components have their respective duties and functions that support the role of blood in the body. To evaluate the overall health and detect such wide range of disorders, including leukemia, infection and anemia, a blood test is conducted. Abnormal increases or decreases in cell counts as revealed in a complete blood count may indicate that people have an underlying medical condition that calls for further evaluation [16]. A complete blood count test is applied to measure several components and features of the blood, including:

Table 1. Blood Types

No	Blood	Role
1	Red blood cells	carrying oxygen
2	White blood cells	fighting infection
3	Hemoglobin	oxygen-carrying protein in red blood cells
4	Hematocrit	the proportion of red blood cells to the fluid component, or plasma, in the blood
5	Platelets	helping with blood clotting

Red blood cells are known to be dark red in color with a huge number of cells in the blood, compared to the two other blood compositions, namely leukocytes and platelets. The presence of hemoglobin, a protein that has a role to bind oxygen in the blood, causes the color of the blood become dark red. In addition to hemoglobin, in red blood cells there is also a hematocrit. Hematocrit measures the proportion of red blood cells to total blood volume which contains both red blood

cells and plasma. Erythrocytes are round with a hollow (biconcave) in the middle [17]. Unlike other cells, red blood cells are easier to change shape to adjust as they pass through the various blood vessels in the body.

Compared to red blood cells, white blood cells make up a substantially smaller percentage of the total blood formation. However, this blood component has a legitimate job to execute, which involves preventing the bacterial, fungal, and viral infections that lead to disease. White blood cells create antibodies that will aid in the defense against these harmful materials, which explains how crucial WBCs are in the blood structure. Adults typically have 3,400–9,600 white blood cells per microliter of blood, with a variety of kinds [17].

Slightly different from white and red blood cells, platelets are not actually cells. Platelets or sometimes also called platelets are small cell fragments. This blood component is also known as platelets. When the body is wounded, platelets play a crucial part in the blood clotting (coagulation) process. Specifically, the platelets will join the fibrin thread to form a plug that will stop the bleeding and encourage the regrowth of tissue around the incision. The normal number of platelets in the blood is between 150,000-400,000 platelets per microliter of blood [17]. If the platelet count is higher than the normal range, it can result in unnecessary blood clots. Finally, it can lead to a risk of stroke and heart attack. Meanwhile, if a person lacks the number of platelets in the blood, it will cause heavy bleeding because the blood is difficult to clot.

Blood plasma is a liquid component of blood. The blood in your body, about 55-60 percent is blood plasma. Approximately 92 percent of blood plasma is made up of water, with the remaining 8 percent being made up of carbon dioxide, glucose, amino acids (proteins), vitamins, lipids, and mineral salts [17]. The main task of blood plasma is to transport blood cells, to be then circulated throughout the body along with nutrients, body waste products, antibodies, clotting proteins (coagulation

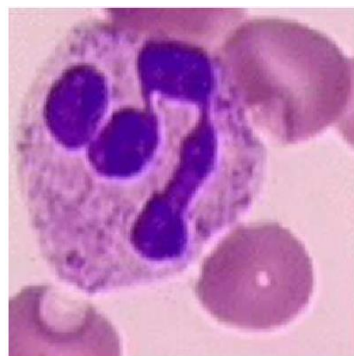


factors), as well as chemicals such as hormones and proteins that help maintain the body's fluid balance. The clotting protein carried by the plasma will work together with platelets as a clotting factor (coagulation) in the blood clotting process. In addition to circulating various important ingredients, blood plasma also functions to balance blood volume and electrolyte (salt) levels, including sodium, calcium, potassium, magnesium, chloride, and bicarbonate.

### **2.2.2. Subtypes of WBC**

Leukocytes or white blood cells play an important role in helping the body fight infection or other diseases. A high leukocyte count can be caused by an infection, but it can also indicate certain diseases to watch out for, such as blood disorders or cancer. Leukocytes or white blood cells are produced by the bone marrow and circulated throughout the body through the bloodstream. Leukocytes are an important part of the immune system that functions to produce antibodies that can fight viruses, fungi, bacteria, and disease-causing parasites that enter the body. Judging from the number, newborns generally have a leukocyte count between 9,000 –30,000 per microliter (mcL) of blood. This range of normal leukocyte counts will change with age to only 5,000–10,000 mcL in adulthood. In adults, the white blood cell or leukocyte count is said to be high if it reaches more than 11,000 mcL [17].

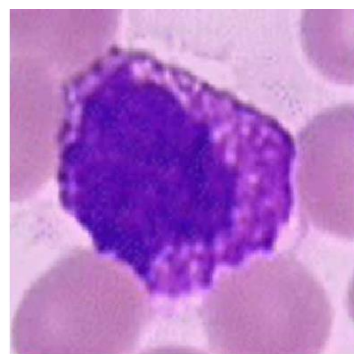
WBC can be used as a material to identify the body's defense activity. Various causes of high leukocyte count when the body's defense system works harder than normally. There are five types of white blood cells or leukocytes, namely neutrophils, lymphocytes, monocytes, eosinophils, and basophils.



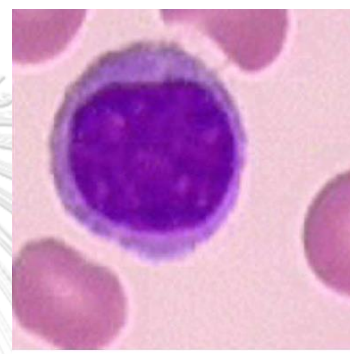
Neutrophils



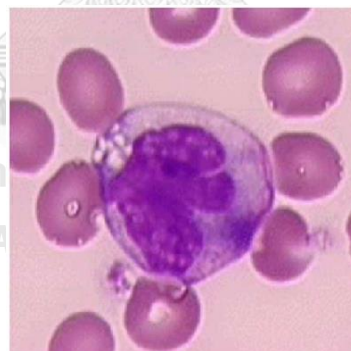
Eosinophils



Basophils



Lymphocytes



Monocytes

*Figure 1 Subtypes of WBC*

When calculated by percentage, leukocytes are called normal if they consist of 40–60% neutrophils, 20–40% lymphocytes, 2–8% monocytes, 1–4% eosinophils, and 0.5%–1% basophils. However, sometimes the number of leukocytes can increase [18].

### 1. Neutrophils

Neutrophils are the most abundant type of white blood cell in the body. Neutrophils can move freely through the walls of blood vessels and into body tissues to fight all bacteria, viruses, and parasites that cause infection [14]. The number of neutrophils can increase if the body experiences several conditions such as bacterial, viral, or fungal infections, and injuries or wounds, for example during postoperative recovery.

### 2. Lymphocytes

There are 2 types of leukocytes, namely B cell lymphocytes which are responsible for producing antibodies and T lymphocytes which play a role in recognizing and capturing foreign organisms or objects in the body. A high leukocyte count can cause an increase in the number of lymphocytes. This condition can be caused by several types of viral infections, such as measles, smallpox, herpes, rubella, cytomegalovirus, etc.

### 3. Monocytes

Among other types of leukocytes, monocytes are the white blood cells with the largest size. This type of leukocyte plays a role in capturing and fighting bacteria, parasites, and fungi that enter the body. An increased number of monocytes can be caused by several things such as infections caused by both viruses such as the measles virus and mononucleosis and bacteria such as tuberculosis, brucellosis, and syphilis.

### 4. Eosinophils

Eosinophils are a type of leukocyte or white blood cell that functions to destroy viruses, bacteria, and parasites, and trigger an inflammatory response, such as in allergic reactions, eczema, and asthma. High eosinophil counts can be caused by

several conditions such as helminth infections, side effects of drugs to hyper eosinophilia syndrome

### 5. Basophils

Basophils are white blood cells that play a role in fighting worm parasites, stopping blood clotting, and producing allergic reactions. High basophil counts can be caused by hypothyroidism, myeloproliferative disease which means disease of the bone marrow, and chronic inflammation such as rheumatoid arthritis and ulcerative colitis [19].

Because it can be caused by many diseases, high WBC is a condition that needs to be treated immediately. To determine the diagnosis of high leukocytes and determine the cause, medical practitioners will perform a physical examination and supporting examinations in the form of blood tests. After the cause of high leukocytes is known, then treatment can be given proportionally.

### 2.3. Machine Learning

Machine Learning (ML) is an approach in AI that is widely used to replace or imitate human behavior to solve problems or perform automation [20]. Machine Learning tries to imitate how humans or intelligent creatures learn and generalize processes. Machine learning applications can be found in various sectors in various forms, one of which is prediction. Machine learning is also a branch of artificial intelligence (AI) and computer science that focuses on using data and algorithms to imitate the way humans learn and gradually increase their accuracy. Machine learning is an important component of the field of science about data development. Through the use of statistics, machine learning algorithms are trained to make classifications or predictions in data development.

Machine learning is also known as part of the domain of computer science with a base of computational mathematics and statistics that can study patterns in data to make predictions about the future. In its development, it is applied by three main methods [21],

### 1. Supervised Learning

The supervised learning method is carried out by labeling the datasets used by machine learning and classified by the developers who encourage the algorithm to see the level of accuracy of its performance. Supervised machine learning in this method is carried out by labeled data which later makes machine learning learn what the relationships and dependencies are between data.

The way this method works is to enter information as input and labeled data as result or output. Input in machine learning, for example, is an image of various objects. The output issued can be in the form of an image detection according to the results of supervised learning.

### 2. Semi-supervised Learning (Unsupervised)

Semi-supervised learning methods can also be referred to as unsupervised machine learning methods. Thus, processes performed on unlabeled raw datasets and machine learning algorithms will try to identify patterns and relationships between data without the help of developers.

In general, unsupervised learning methods do not require any assistance from humans so that computers can study data in effect and their relationships independently. In this case, the dataset is unlabeled, and the machine will computationally identify patterns in the data. Unsupervised learning is used to make it easier for developers to make decisions.

Unsupervised learning can automatically search for information after grouping patterns from all the data that has been studied.

### 3. Reinforcement Learning

This machine learning method is run using a “rewards/punishment” system dataset and offers feedback to the algorithm to learn from its experience on a random basis. This "trial and error" method is almost the same as the pattern understanding system used by humans, namely learning from experiments.

This is what makes this method known as machine learning with the type of learning reinforcement. The algorithm in this method will learn continuously from the environment or interaction habits associated with it. From there, the algorithm will get "rewards" or "punishments" as positive and negative impressions based on the

experimental actions. This algorithm is usually developed for game application development.

## 2.4. Convolutional Neural Network (CNN)

There are various neural network proposes by researcher and enterprise company recently. Some surveys also conducted to compare their performance as a study. Stanford University [22] recently made available the most recent dawn benchmark results. Huawei cloud modelarts scored top in terms of the overall training time for image recognition of ResNet50 on Imagenet [23], with 93 percent accuracy or above, only needing 10 minutes and 28 seconds, or roughly 44 percent less time than the second. That outcomes demonstrate that Huawei cloud modelarts has achieved a more affordable, quick, and extreme experience.

Alex Krizhevsky [24] proposed the ImageNet Large Scale Visual Recognition Challenge 2012 with development method for his CNN. This achievement proves that the CNN method has outperformed other Machine Learning methods in the case of object classification in the image. The CNN method is a development of the Multilayer Perceptron (MLP) which is constructed as in Figure 2 to process two-dimensional data. The way CNN works is similar with MLP, but in CNN each neuron is represented in three dimensions, unlike MLP where each neuron is only one-dimensional [25].

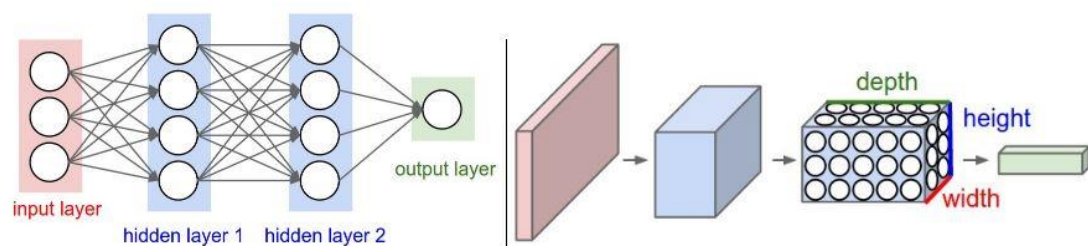


Figure 2. MLP Dimension (left) and CNN (right)

There are CNN architectures that are commonly used. The architectures are AlexNet, VGGNet, GoogLeNet and ResNet. It can be seen in the example of CNN architecture in Figure 3, CNN consists of three layers which are convolutional layer

(Conv), pooling layer (Max pooling) and fully-connected layer (Full Connection). These layer stacks build the architecture of the CNN.

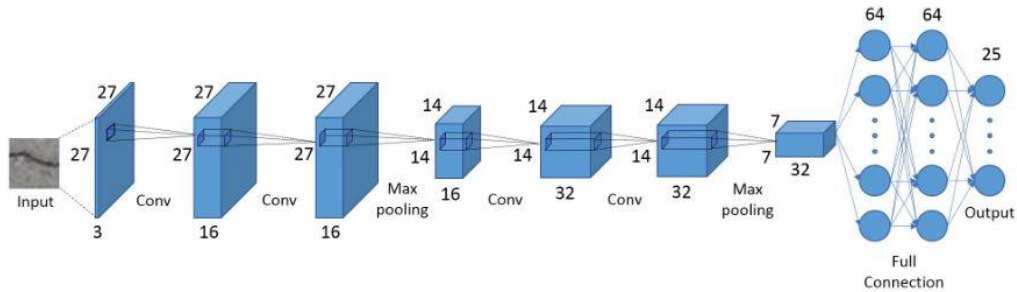


Figure 3. An Example of CNN Architecture

The basic functions of CNN above can be explained into four main areas, namely [26]:

a) Input layers is the layer which will store the pixel values of the input image. Figure 4, the size of the input data is  $27 \times 27 \times 3$ , meaning  $27 \times 27$  is the image pixel size and 3 is the number of image channels, namely Red, Green, and Blue.

b) Convolutional layers is the layer which will explore the output of the neurons connected to the input layer by calculating the product scalar between the weights and the area connected to the input. Illustration of the process in the convolutional layer can be seen in Figure 5. In this illustration, zero padding is used, which is the addition of 1 line of zero values along the input boundary line. In the convolution process, a Rectified Linear Unit (ReLU) is used to apply an 'element wise' activation function as well as sigmoid to the output of the activation generated by the previous layer, the ReLU graph, which is shown in Figure 6.

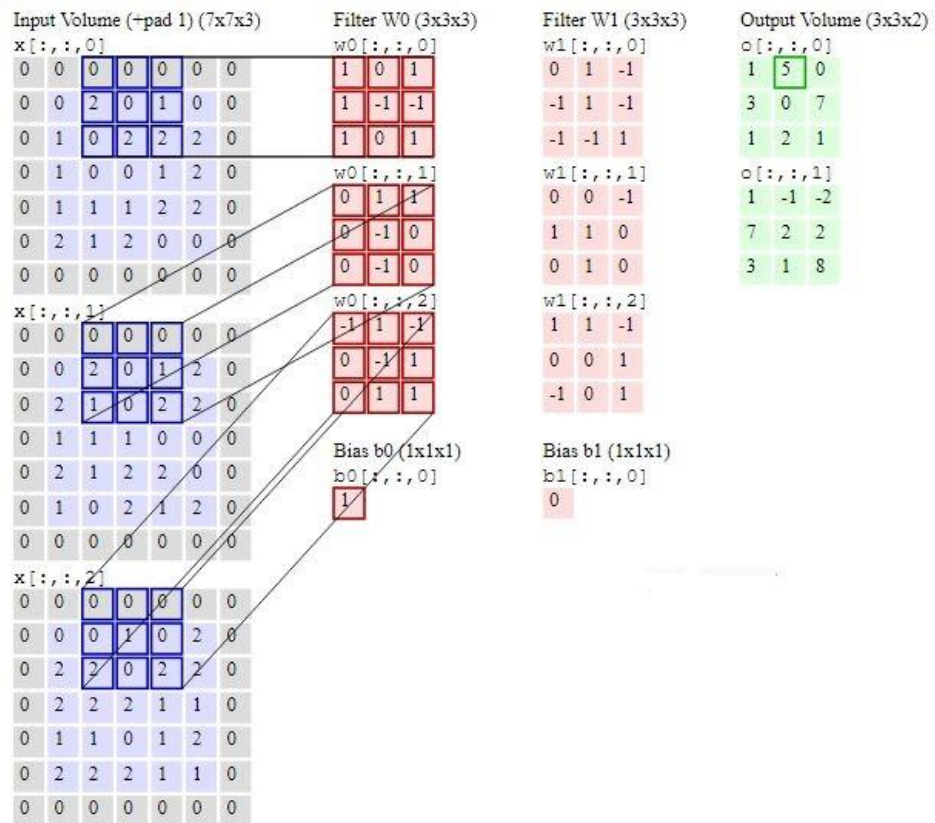


Figure 4. Convolution Process

$$f(u) = \max(0, u)$$

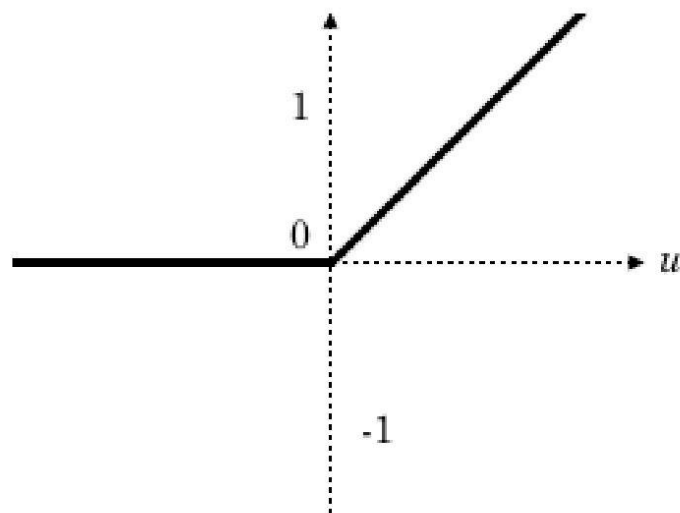


Figure 5. ReLu Activation

c) Pool layer will execute down sampling on the trough the spatial dimension of the given input, then reduce the amount of parameters in the



activation. Pool layer operates an activation map to all inputs and uses the "MAX" function. In most CNNs, the max-pooling layer uses a kernel with dimensions of  $2 \times 2$  with a stride of 2 along the input spatial dimensions, meaning it moves by 2 steps in its kernel movement. This causes the input size to decrease to 25% of its original size. An illustration of this mechanism is presented in Figure 6. This illustration uses a kernel with dimensions of  $2 \times 2$  with stride 1.

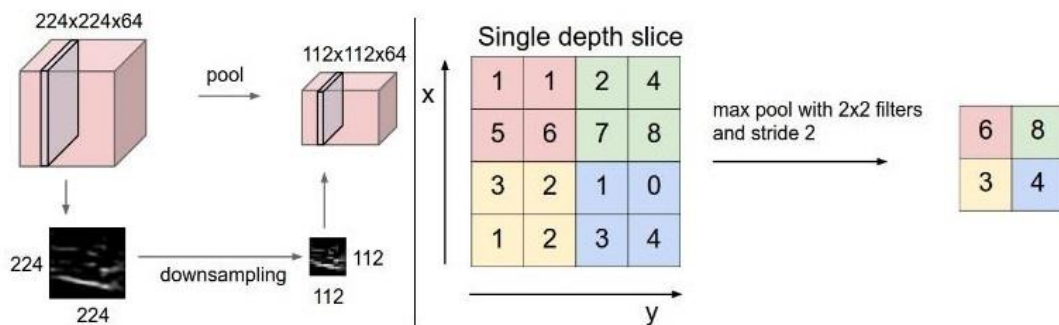


Figure 6. Max Pooling

d) Fully-connected layer. This layer will perform the same task as a standard Neural Network and attempt to generate a class value from activation, which is used for classification. This layer is in line with the way the neurons are organized in the ANN.

## 2.5. YOLO (You Only Look Once)

### 2.5.1 Object Detection

Computer vision is applied recently in many fields as an interdisciplinary study. It has impacted as well as CNN application. It is applied in many sectors like self-driving cars in the foreground. Object detection is another essential consideration of computer vision. Motion prediction, object recognition, and surveillance systems gain all benefits from object detection. Object detection algorithms differ beyond classification algorithms in that detection algorithms attempt to draw a bounding box around the target object in order to locate it within the image. Additionally, in an object detection circumstance, users may not sketch just one bounding box. There can be numerous bounding boxes representing separate objects of interest within the image, and it is not able to be known the number exactly.

Currently, in detecting an object, the system operates a classifier and evaluates the object at several locations and scales within the image. The DPM (Deformable Parts Model) system adopt a sliding window technique where classes are run evenly throughout the image. Meanwhile, R-CNN (Regional Convolution Neural Network) uses the regional proposal method to firstly generate a potential bounding box in an image, and then run a classification for the proposed bounding box [27]. After classifying, post-processing is utilized in filtering bounding boxes, eliminating duplicate object detection, and comparing prediction boxes against other objects. This complex flow takes a long time and is difficult to optimize because each component has to be trained separately. YOLO makes the object detection process as a single regression problem, processing directly from image pixels to bounding box coordinates and class probabilities. By using YOLO, the system only looks once (You Only Look Once) on the image to detect and predict what objects are there and where they are [28].

### 2.5.2. Architecture

YOLO combines jointly the separate components of object detection into a neural network. YOLO utilizes a tour of the entire image to predict each bounding box. YOLO predicts all bounding boxes on all object classes for an image at the same time. This means that YOLO considers all parts of the image globally and all objects in the image. YOLO divides the input image into  $S \times S$  tiles (grids). If the center of the object is in a tile, the tile cell is responsible for detecting that object.

Each tile cell predicts  $B$  bounding boxes and confidence values for those boxes. This confidence value reflects how sure the box contains the object as well as how accurately the predicted box is. YOLO formally defines trust as  $\Pr(Obj) * IoU_{pred}^{truth}$ . If there is no object in that cell, the confidence value must be zero. Otherwise, the confidence value will be equal to the intersection of union (IoU) between the predicted box and the ground truth box.

Each bounding box consists of 5 predictions:  $x, y, w, h$  and a confidence value of  $p$ . The coordinates  $(x, y)$  represent the center of the grid relative to the tile cell

boundary. Width ( $w$ ) and height ( $h$ ) are predicted relative to the entire image. Finally, the predicted confidence value states the IoU between the predicted box and the ground truth box.

Each tile cell also predicts the conditional class probability as  $C, Pr(Class_i|Object)$ . This probability is conditioned on the tile cell that contains the object. YOLO predicts a set of class probabilities per tile cell, regardless of the number of squares  $B$ . During the experiment, the conditional class probabilities are multiplied by the individual box confidence predictions which give a class-specific confidence value for each box, and is shown in equation (1) below,

$$Pr(Class_i|Object) * Pr(Object) * IoU_{pred}^{truth} = Pr(Class_i) * IoU_{pred}^{truth}, \quad (1)$$

This value encodes the probability of the class appearing in the box and how well the predicted box fits the object. The illustration of the model can be seen in Figure 7. YOLO applies this model as CNN. The initial convolutional layer of the network extracts features from the image while the fully-connected layer predicts the probabilities and output coordinates.

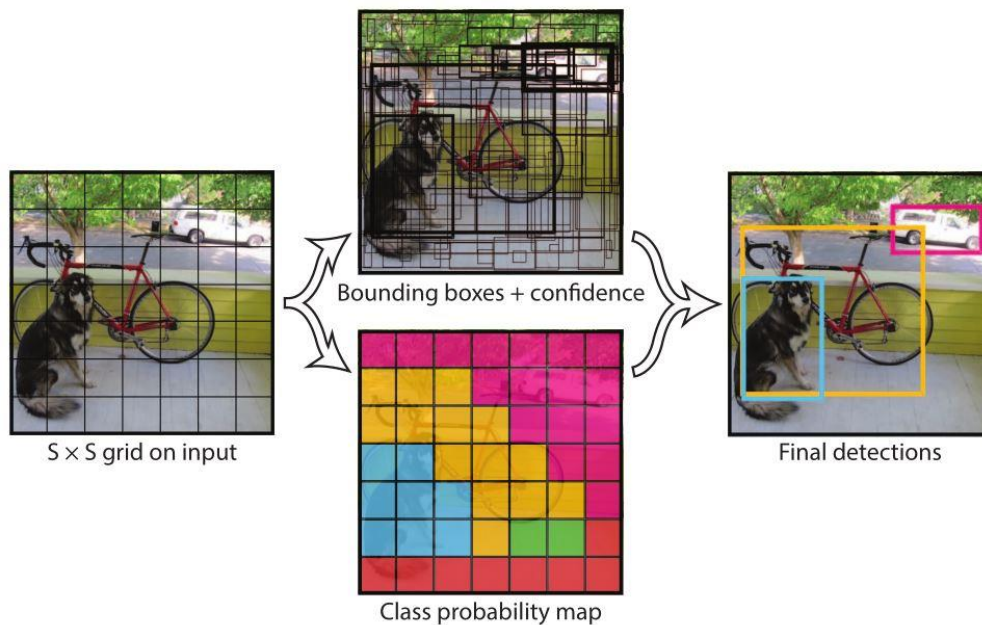


Figure 7. Model YOLO  
(Redmon et al., 2016)

YOLO has been continuously developed since the model was first built. The basic version of YOLO has 24 convolutional layers followed by 2 fully connected layers. This architecture uses a  $1 \times 1$  reduction layer followed by a  $3 \times 3$  convolution layer. YOLOv3 is based on Darknet Architecture and features 53 layers that have been trained on the ImageNet dataset [23]. Upsampling and residual connections are used in YOLOv3. At three distinct scales, the detection is carried out. Although it is more effective at recognizing smaller objects, it takes longer to analyze than earlier versions [22]. The CSPDarknet53 backbone, spatial pyramid pooling extra module, PANet path-aggregation neck, and YOLOv3 head make up the YOLOv4 architecture. The backbone of the YOLOv5 model is a Focus structure with a CSP network. The SPP block and PANet make up the neck. It uses GloU-loss and has a YOLOv3 head. The latest version of YOLO is written in Python, whereas prior versions is written in C. This simplifies the process of installing and integrating IoT devices.

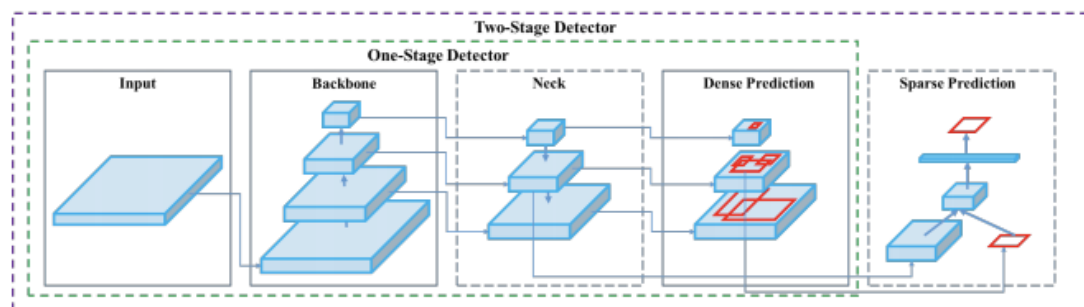


Figure 8. The YOLO object detection process

YOLOv5 is made up of three parts: (1) CSPDarknet is the backbone, (2) PANet is the neck, and (3) Yolo Layer is the head. The data is first supplied into CSPDarknet, which extracts features, and then into PANet, which fuses them. Finally, Yolo Layer gives you the results of your detection (class, score, location, size) [29]. As a comparative study in the implementation of the YOLOv3, YOLOv4, and YOLOv5 algorithms, Sahla Muhammed Ali [30] implements those to train the sign language dataset. The precision, recall, and accuracy of the results from each algorithm were determined. When the accuracy values and results from the three versions are compared, the best version is YOLOv5.

### 2.5.3. Performance

The steps for working on the basically YOLO method can be seen in Figure 9, where the Convolutional Neural Network (CNN) simultaneously predicts several bounding boxes and class probabilities for those boxes. YOLO trains the entire image and optimizes detection performance in real-time. This integrated model has several advantages over traditional object detection methods.

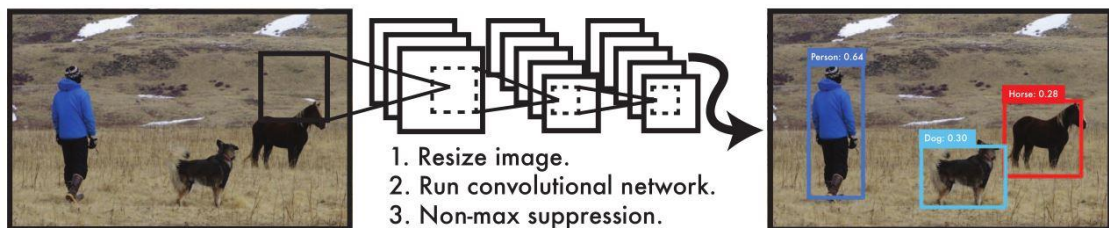


Figure 9. YOLO Detection System

(Redmon et al., 2016)

First, YOLO is very fast. Because YOLO makes object detection a regression problem, so it doesn't require complex paths. YOLO only runs CNN on the image to predict detections. YOLO can process video streams in real-time with less than 25 milliseconds of latency and achieves more than double the MAP (Mean Average Precision) of other real-time systems.

Second, YOLO considers globally about the current image make predictions. Unlike sliding window and region-based proposal techniques, YOLO looks at the entire image during the training and testing period so that it implicitly encodes contextual information about the class according to the object displayed in the image. Fast R-CNN, the best detection method, has an error in detecting the background in the image for objects because it cannot see the larger context. YOLO makes less than half the number of background errors compared to Fast R-CNN.

Third, YOLO can learn to generalize object representations. When trained on natural images and tested on the artwork, YOLO outperforms the best detection methods such as DPM and R-CNN by a wide margin. Because YOLO is highly

generalized, it is more likely to break when applied to new domains or unexpected input [28].



## CHAPTER 3 METHOD

### 3.1. Data Acquisition

Data acquisition is the most fundamental stage in this study. A number of datasets in images of subtypes of WBC are captured manually under a lens of a microscope. A machine vision device is integrated with a microscope to take the observed images. The capturing process for the image considers the size of the lens, and focuses in the process of operation. The slide containing the blood sample, having been installed, is shifted both vertically and horizontally to get the number of objects that can be observed thoroughly with a variety of sampling techniques. This process will produce raw blood samples that have not been given any treatment which will be used as the main dataset. This dataset has the sample of subtypes of WBCs in the form of neutrophils, eosinophils, and basophils, monocytes, and lymphocytes.



*Figure 10. Data Acquisition Using Microscope*

This research involves collaborative researcher from Faculty of Medicine. The discarded slides are clinical specimens that are normally discarded after 1 month. The tags of slides will be removed. Therefore, the patient identities are not revealed. This research uses the leftover human samples without collecting the blood samples from any volunteer. These slides are obtained from Prof. Dr. Ponlapat Rojnuckarin

([Ponlapat.R@Chula.ac.th](mailto:Ponlapat.R@Chula.ac.th)) as cooperative researcher from the Division of Hematology, Department of Medicine, Faculty of Medicine, Chulalongkorn University.

### 3.2. Data Augmentation

The limitation of the dataset in this method encourages this study to do data enrichment properly. This model has three main parts. The first model is built based on training data using raw data taken from the microscope instantly. The second part is a model constructed with a combined dataset of raw data and data enrichment through augmentation techniques based on geometric operation. This data augmentation is conducted with several methods with the number of images where the technique utilized is based on geometric operations by performing rotation, translation, horizontal flip, and magnification. Several stages are proposed in this section by some steps in Figure 11.

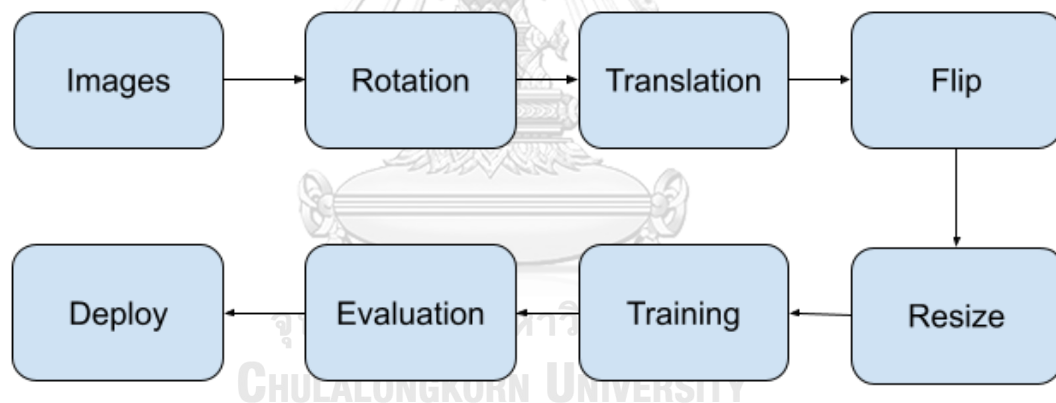


Figure 11. Augmentation based on Geometric Operation

And the third is the accumulation of the original image with the augmented data based on image enhancement procedures. Image enhancement is the process with some procedures of improving the quality and information of original images. This process has several techniques of enhancing the original data content before processing. This research applies these methods to imitate the real problem while the process of microscopy object is performed. This augmentation method performs contrast enhancement, gaussian noise, brightness enhancement, motion blur and



disk blur. Several stages are proposed in this section by some steps in Figure below. We precisely present the appurtenant solution of sub-types of WBC detection.

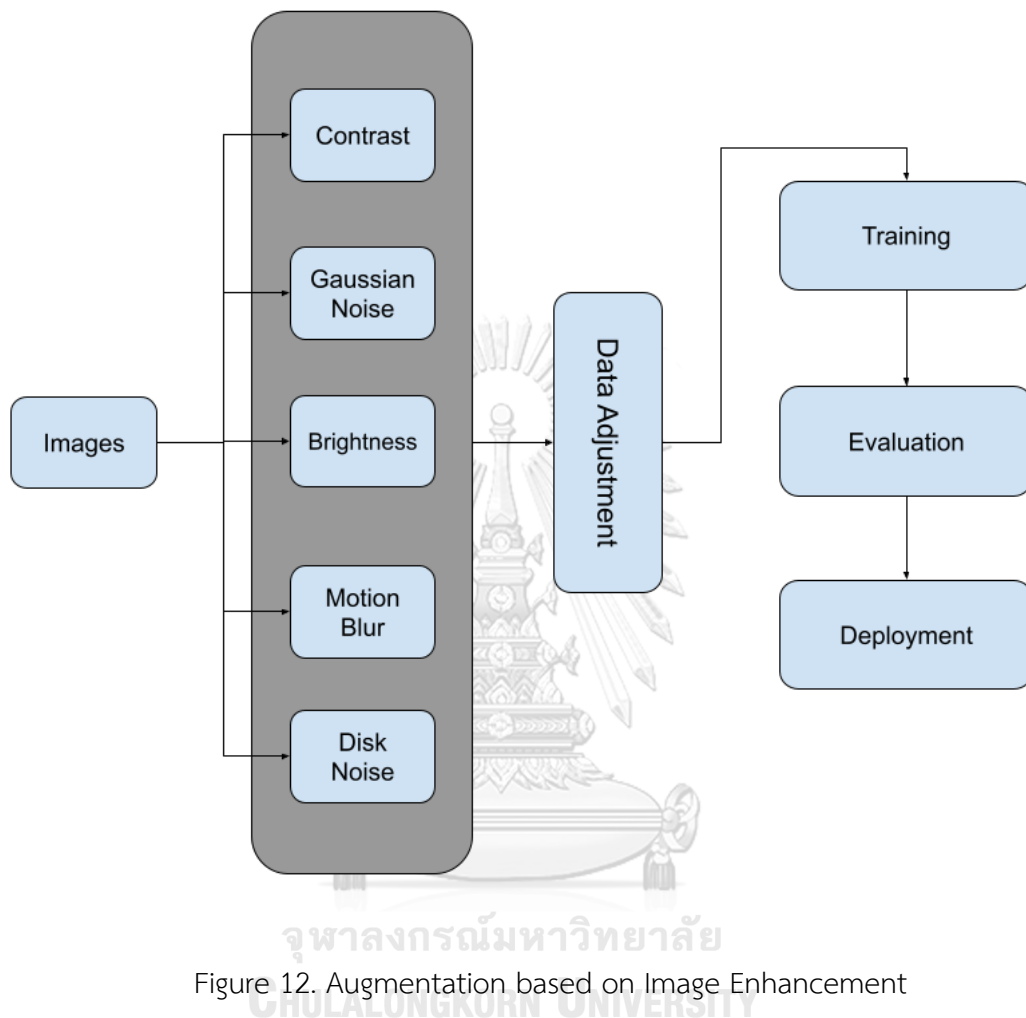


Figure 12. Augmentation based on Image Enhancement

### 3.3. Data Splitting

The data splitting step is the process to divide the total data for the training process and validation test. The data used for training are as much as 80% while for validation test data as much as 20% of the total data. The amount of data collected previously is divided to all of subtypes of WBC. The training data is grouped in a train folder and testing data is collected to a test folder.

The sample sizes of training data and test data are 80% and 20%, respectively. Based on some literatures conducted in previous studies, the size of the sample is expected to be fine by applying that ratio [31], to get good result, approximately 500

images are needed for each class to yield good accuracy. Thus, the minimum dataset used for the 5 subtypes of WBC comprise 2500 images. This number is subject to change because of model development adjustments are usually required during model development. In case of YoloV5 usage, at least 1000 dataset each class is suggested to use when the result is not enough satisfactory [32].

The function of training is to train the model to recognize patterns in the data, while testing is to ensure that the model that has been trained is able to predict the labels of new observations and has not been studied by previous models. According to some resources, the comparison of the sizes of the training and testing data vary but most developers use a ratio of 80% and 20% because the results are satisfactory and safe from over fitting [33]. The other ratios while in other cases the comparison is used like 75% and 25% or 70% and 30% have also been reported. In the biomedical field, the remarkable result is achieved in using YoloV5 with ratio 80% and 20% respectively on abnormalities detection [34].

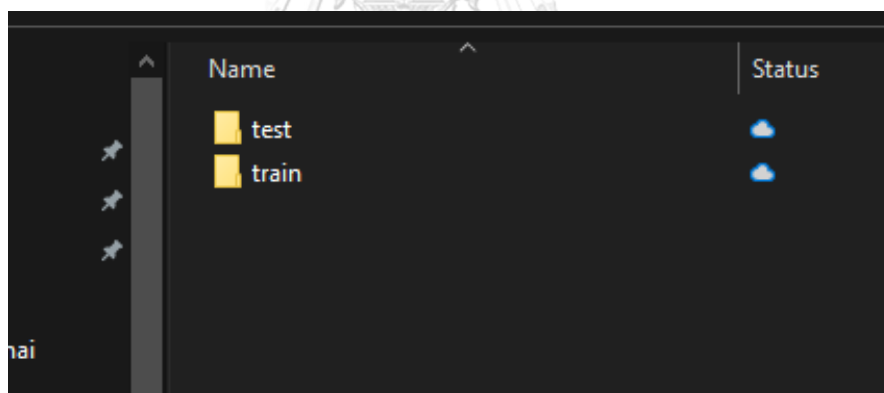


Figure 13. Data Splitting

### 3.4. Data Annotation

The data annotation stage is the step of providing information on each image data. The information is in the form of coordinates, the confidence level of the bounding box and the type of subtypes of WBCs contained in the image. This information will be used for the training and testing process. This stage uses an open-source tool in labeling images.



Figure 14. Data Annotation

### 3.5. Design and Implementation

This proposed study proposes the application of Design and implementation of subtypes of WBCs detection applications. Different complexity and datasets will produce various results. According to experimental findings, the smaller model from ShrimpNet-3 which is the improved model by Liu et al. [35] could validate the created dataset with an accuracy of 96.84 percent and in 0.47 hours. The proposed method is therefore promising for classifying shrimp and measuring the quality of production lines. In this study, the method used to detect and count the subtypes of WBCs using YOLOv5 family model with different version and complexity which can be used open source. So, it is necessary to adjust the hardware and software requirements in implementing YOLOv5 for the dataset used in this study. The model will be trained with 16 batch size and 600 epochs.

### 3.6. Testing and Evaluation

The testing process is carried out by conducting a model testing process by testing it with several the image variations. The testing process is carried out to determine the performance of the model in recognizing the object being tested. The evaluation of model performance is defined by comparing the actual value with the predicted value. Confusion Matrix is a performance measurement for machine

learning classification problems where the output can be two or more classes. Thus, the accuracy value of the built detection system can be defined.

The verified dataset is applied to develop the models. There will be at least 2 models developed in this research. The model that is built will have different performance because it has different augmentation techniques and neural networks. Every model built will be tested. As in performance testing on machine learning model development, in this study the model will be evaluated with a confusion matrix.



## CHAPTER 4 RESULT AND DISCUSSION

### 4.1. Data Collection

Data collection is the most essential stage before building a model to detect objects. To detect objects with good performance, a data set is required which is qualified according to the class specification. In this study, researchers collected data independently by observing blood using a microscope. Objects are captured using a module that has been developed, namely MicrosisDCN [36].



*Figure 15. MicrosisDCN Module*

The MicrosisDCN module was developed based on the Raspberry Pi. Supported with EagleEye (Smart Camera), this module has strong performance in object inspection process. Based on the Raspberry Pi CM3+, this module is supported by 16 GB of memory with a 1.2 GHz CPU and 1 GB of RAM. These specifications illustrate that this module is very good for light and flexible work.



Figure 16. MicrosisDCN for Image Capturing

In the aspect of image capturing, a 5MP Full-HD Image Sensor is embedded in the module. Specifically designed for inspection of microscopic objects, the MicrosisDCN has a 4mm/12mm/5-50mm Lens CS mount. The embedded camera is used for general image capturing purposes. The lens slot provided is used for the need for observation using a microscope. Using the device that was built, the image observation process can be done more concisely. This device is supported by the miniHDMI to HDMI cable, LAN cable, and USB 2.0 features that make it easier for users to observe objects using the screen as well as using a personal computer.

CHULALONGKORN UNIVERSITY

Table 2. MicrosisDCN Specification

<p><b>Specification:</b></p> <p>EagleEye (Smart Camera)</p> <p>Raspberry Pi CM3+</p> <p>Image Sensor 5MP Full-HD</p> <p>Lens CS mount as 4mm/12mm/5-50mm</p> <p>Power Supply Industrial 24V 2A</p> <p>miniHDMI to HDMI cable</p> <p>LAN cable and USB 2.0</p>
---

EagleEye Flasher CM3+ board  
 Full size heat sink and enclosure  
 Software Dev Kit API for Python/C++ for OpenCV  
 OS Embedded Linux RT for Machine Vision

The Raspberry Pi is a single-board computer that has been flexible and reliable to date. It can be applied for various purposes such as desktop PCs, home media centers, to automation systems. Installing the Raspberry Pi operating system is the initial stage in preparing supporting software in the image capturing process for observing microscopic objects in this research topic. Installing the Raspberry Pi operating system can be executed by writing the OS image file to the SD card and then installing it on the Raspberry Pi board. There are two main files that must be prepared in the installation process of this operating system, namely (1) Raspberry Boot Loader and (2) Raspberry Imager.

Table Table 3. Raspberry Pi OS Installation

Tools	Source
(1) Raspberry Boot Loader	<a href="https://www.raspberrypi.com/documentation/computers/compute-module.html">https://www.raspberrypi.com/documentation/computers/compute-module.html</a>
(2) Raspberry Imager.	<a href="https://www.raspberrypi.com/software/">https://www.raspberrypi.com/software/</a>

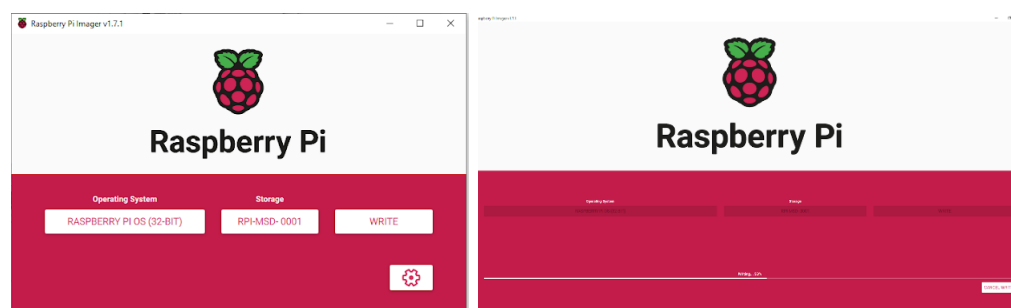
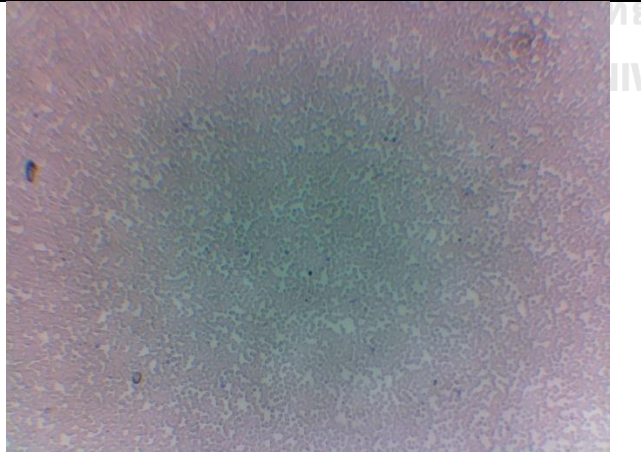



Figure 17 . Installation Process for Raspberry Pi OS

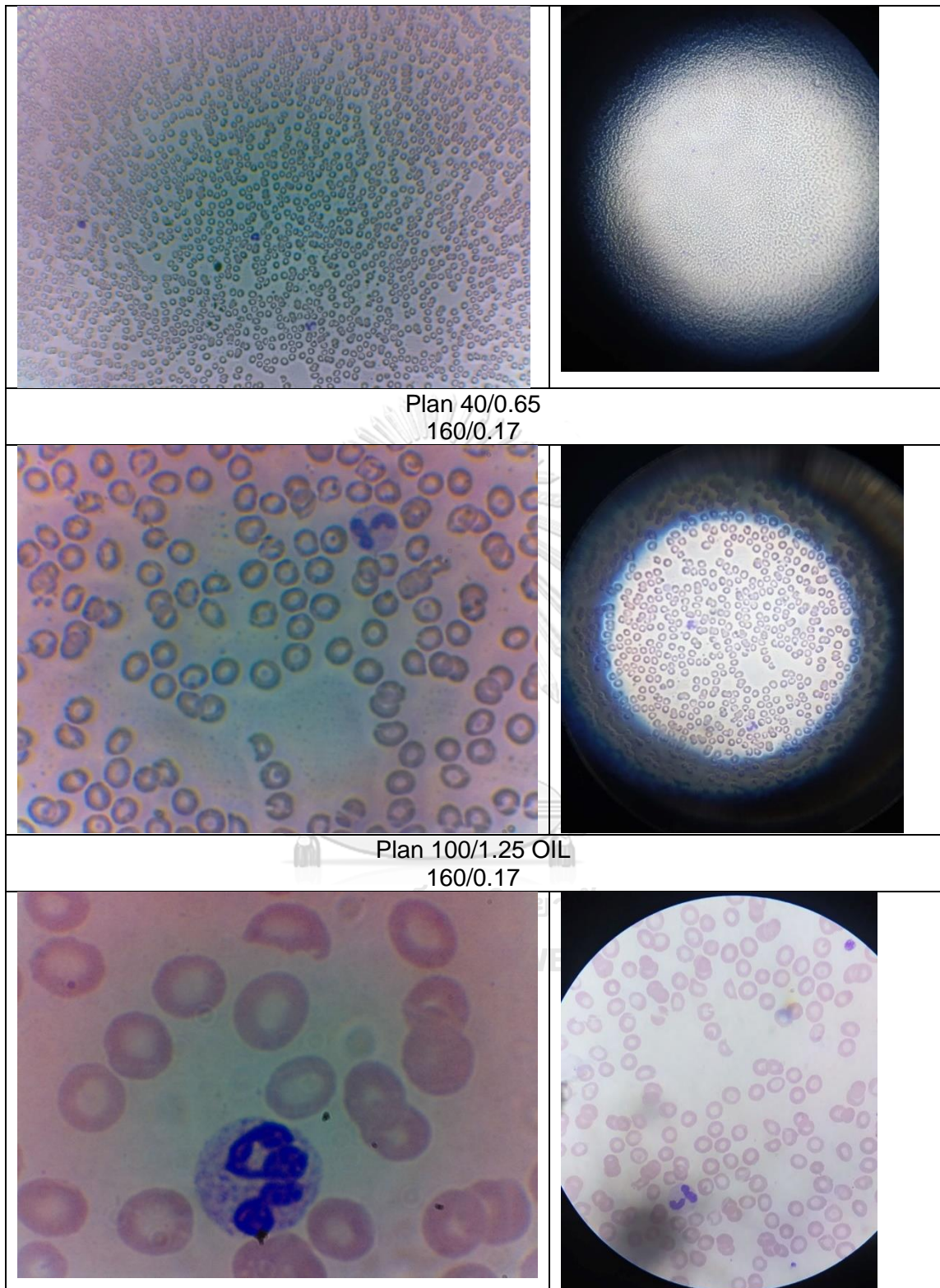
Image capturing in this study begins with observing blood with a microscope using several variations of the size of the objective lens where there are 4 sizes to choose from. The objective lens is the lens that is close to the object. The microscope used has 4 objective lenses on the microscope, namely by choosing a magnification of 4, 10, 40, or 100 times. When using the objective lens, the observer must apply immersion oil to the object, this immersion oil serves as a lubricant and to clarify the image of objects, because at 100 times magnification, the location of the lens with the object being observed is very close, sometimes even touching.

Images of blood samples taken using MicrosisDCN are compared with respect to the selected magnification. The clarity of the observed object is considered for later use as a candidate dataset. The image capture method on MicrosisDCN uses the terminal by entering the command "`raspistill -o plan-x.jpg`" using the one used for image capture. "`raspistill --timelapse 6000 --quality 100 --width 1440 --height 900 --output /home/pi/capture/plan 40/img%04d.jpg --exposure auto -v -t 999999999`".

Table 4. Data Observation

Captured by MicrosisDCN	Captured by Xiaomi Redmi Note 8
Plan 4/0.10 160/0.17	
	
Plan 10/0.25 160/0.17	

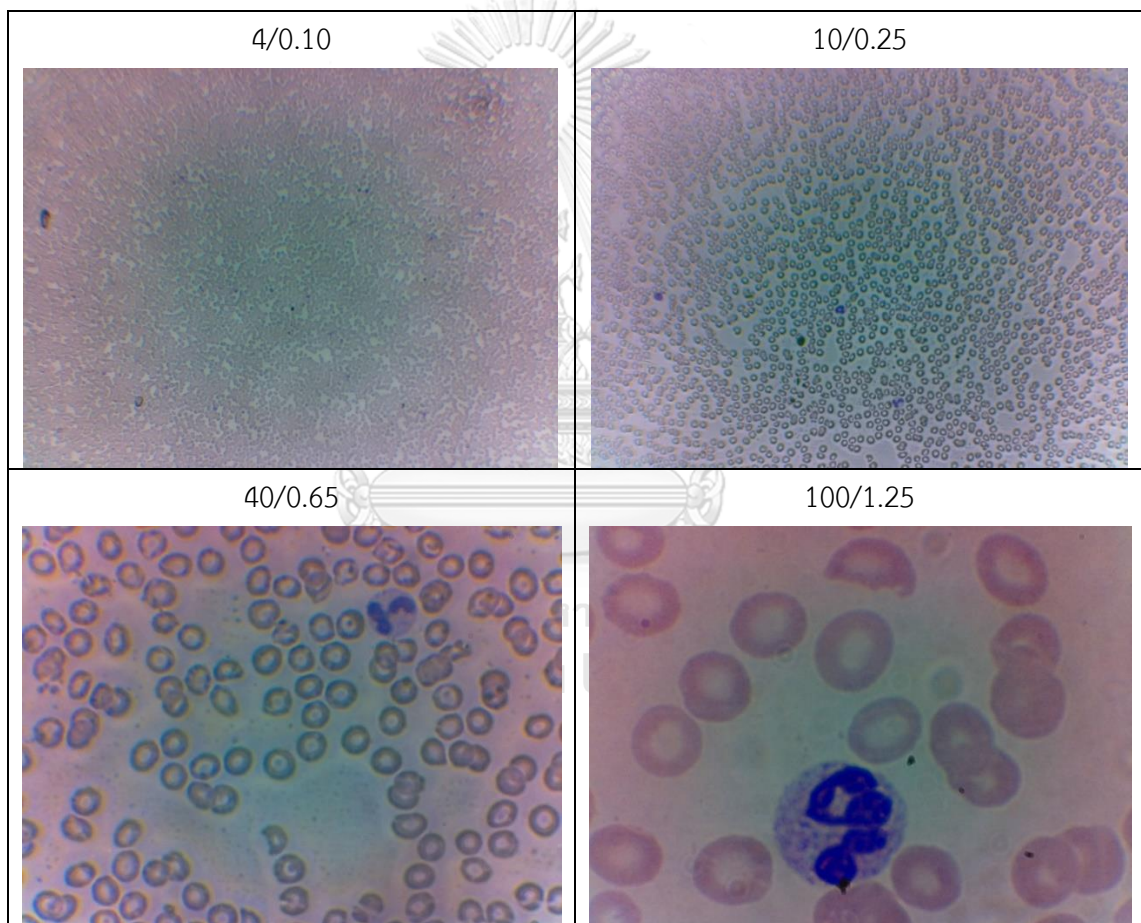




The observation stage is based on the four types of objective lenses used, this study decided to use an objective lens with a plan magnification of 40/0.65

(160/0.17). The 40 magnifications is chosen because it has good visibility where the white blood cell image can be distinguished according to the 5 subtypes to be detected. Images observed using objective lenses with magnifications of 4 and 10 look too small and have low visibility. While the objective lens with a magnification of 100 has very good visibility, but the object looks too large so that the scanning and capturing image process takes a long time.

*Table 5. Captured Images with Different Magnification*



In this study, researchers collaborated with a pathologist as a collaborative researcher from the Faculty of Medicine, Chulalongkorn University. This collaboration is an important point in this study where the researcher is not an expert in the field of hematology. The collaboration that was built between researchers and collaborative researchers was to verify the data collection and selection process.

Collaborative research is part of the research process where this research has been approved by the Ethics Review Committee, Chulalongkorn University and can be done legally.

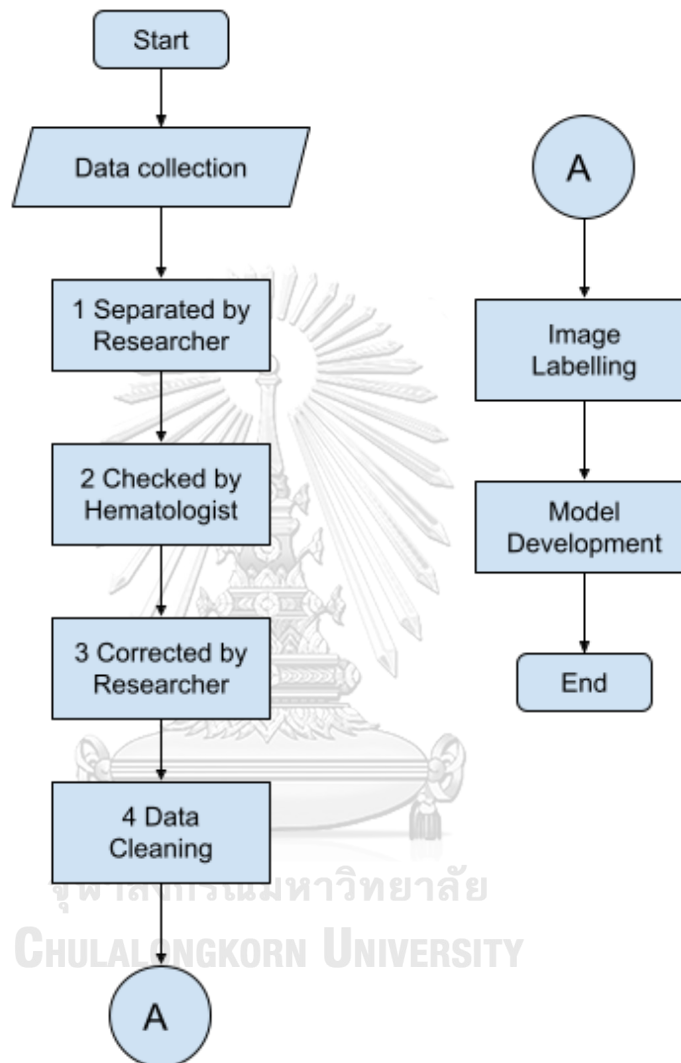


Figure 18. Data Verification

Data verification is an important stage before building a model. In the data verification process, there are 4 stages before finally carrying out the labeling process. After the image is taken with a scanning technique in the observation process using a microscope and MicrosisDCN, first the image will be separated by researchers based on their respective subtypes. The second stage, the hematologist as a collaborative researcher verifies the classification in the first stage that has been carried out by the

researcher. Third, the researcher will reclassify based on the comments and verification given by the collaborative researcher. Finally, the images that have been selected by going through stages one, two and three will be re-selected by considering the level of visibility and image quality. After going through all these stages, the image is processed using the Labeling Tools to provide notation.

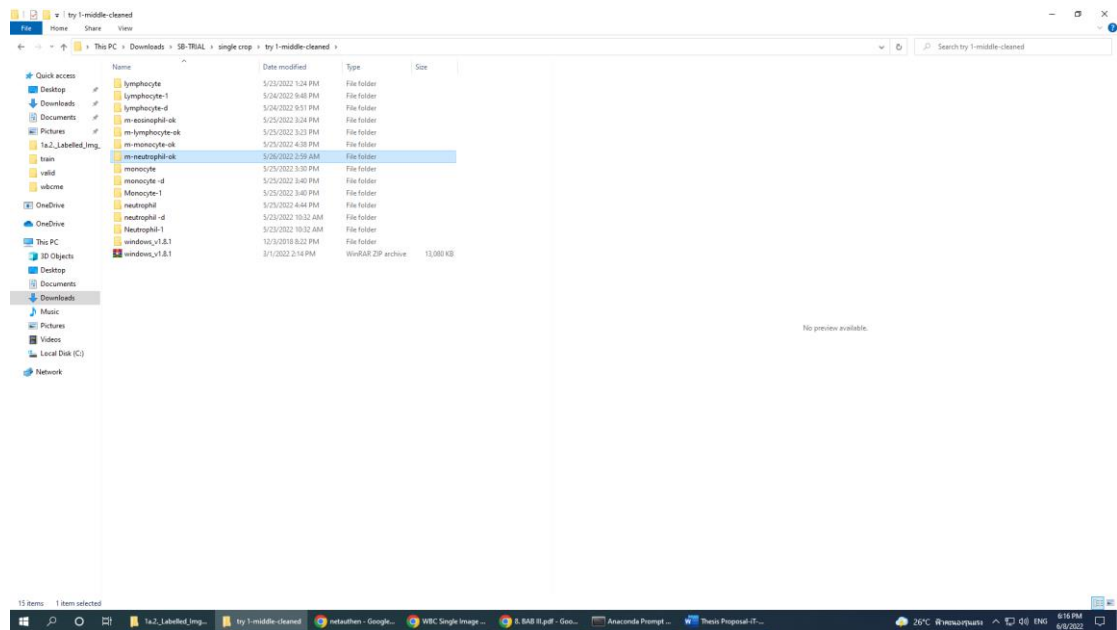


Figure 19. First Grouping

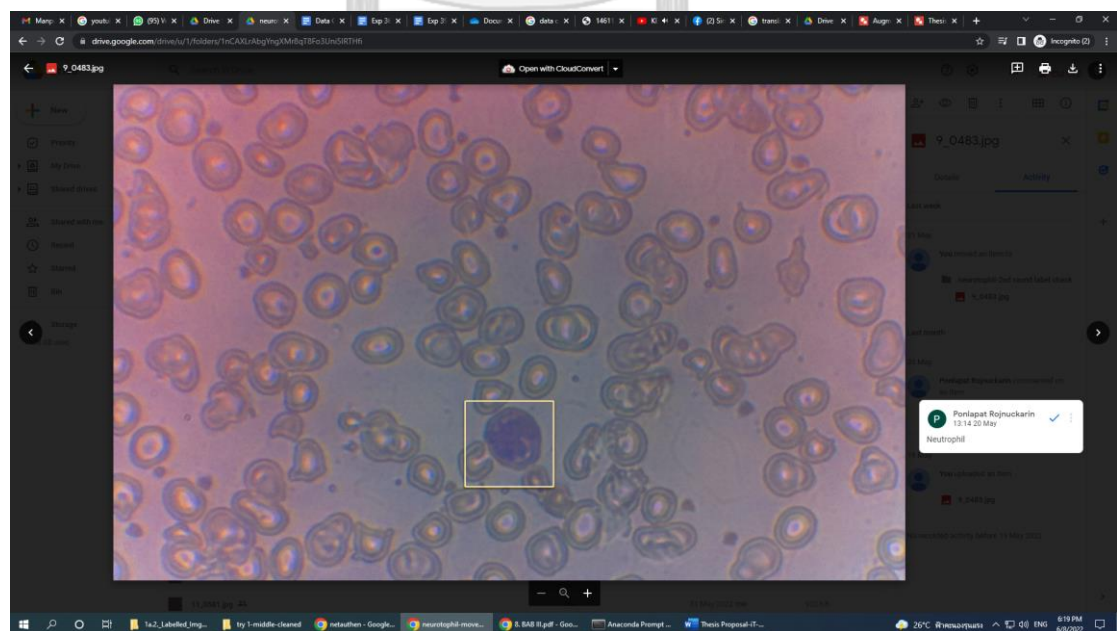


Figure 20. Data Verification

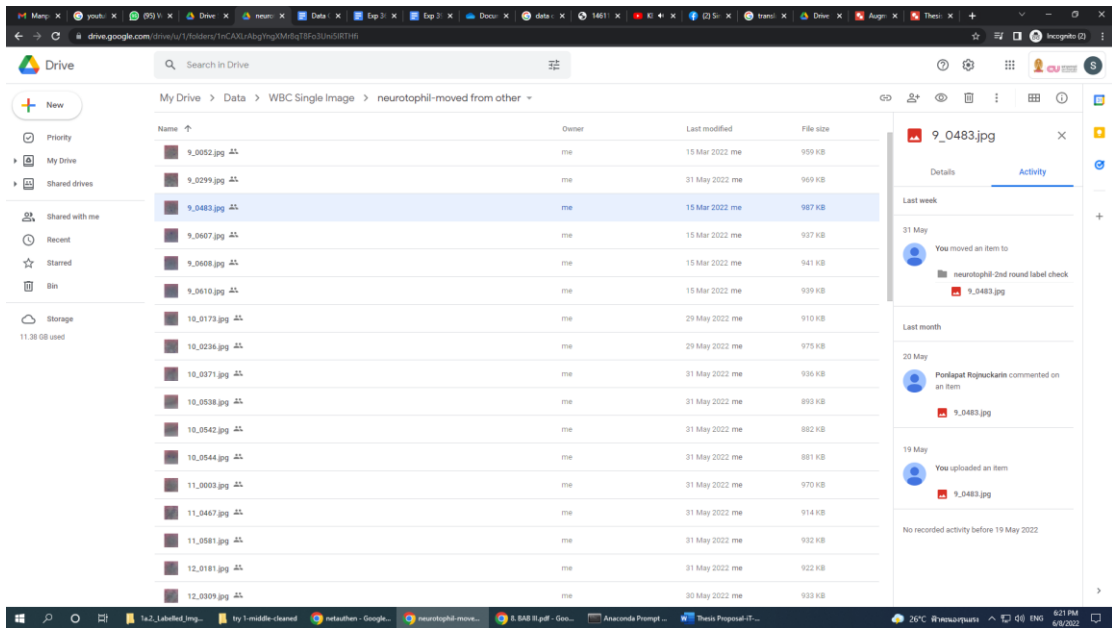


Figure 21. Data Correction

Finally, from several steps passed by the dataset can be defined. The raw data is captured using MicrosisDCN which has several imbalance data naturally. It has been supported by some mechanisms to obtain more images specifically. Therefore, the amount of raw data for neutrophil, eosinophil, basophil, lymphocyte, and monocyte is 603, 109, 179, 384 and 163 respectively. The dataset is split with ratio 80:20. Therefore, training data for neutrophil, eosinophil, basophil, lymphocyte, and monocyte is 482, 87, 143, 307, and 130 respectively. So, testing data for neutrophil, eosinophil, basophil, lymphocyte, and monocyte is 121, 22, 36, 77, and 33 respectively.

Table 6. Raw Data

No	Classes	Sample	Train	Test
0	Neutrophil	603	482	121
1	Eosinophil	109	87	22
2	Basophil	179	143	36
3	Lymphocyte	384	307	77
4	Monocyte	163	130	33

## 4.2. Image Augmentation

The minimal amount and variety of data used to build models using neural networks can be overcome by data augmentation processes. This technique aims to produce more varied data. This process can also shorten the time in the data acquisition process where in this study the data was taken directly using a microscope with the MicrosisDCN device. This study examines two types of image augmentation based on geometric operations and image augmentation based on image enhancement.

### 4.3.1. Geometric Operation-based

Initially, the WBC subtypes ( $I_b^t$ ) are selected with several images ( $N_t$ ) as in (2). The number of datasets in each class ( $N_t$ ) is estimated with the target ( $N_{ET}$ ) to determine the multiplication factor ( $m_b^t$ ) as in (3). This procedure-repeated is adopted for all subtypes of WBC to determine the set of multiplication factors ( $m_b$ ) which describes the number of enlarged images that is produced from each image (n) of a particular subtype of WBC. The rotation R as ( $\theta^\circ$ ), flip (HF), translation (T) and magnification vector (RZ) are selected specifically and measured according to the predetermined values to produce an augmented set ( $I_{ab}^{nt}$ ) image using a single image ( $I_b^{nt}$ ) as in (4). Finally, all augmented images ( $I_{ab}^{nt}$ ) are added up with the original images ( $I_b^t$ ) to produce new datasets ( $I_{Nc}^t$ ) as in (5) with a nearly balanced sample size across the subtypes of WBC,

$$I_b^t \{I_b^{1t}, I_b^{2t}, \dots, \dots, I_b^{nt}\}, \quad (2)$$

$$m_b = \{m_b^t = \left\lfloor 1 - \frac{N_t}{N_{ET}} \right\rfloor, t \in [1, 2, \dots, T], N_t < N_{ET}, \quad (3)$$

$$I_{ab}^{nt} = \{H(I_b^{nt}, \theta_a, FH_a, T_a, R_a, FV_a) \mid a \in [1, 2, \dots, m_b^t]\} \quad (4)$$

$$I_{Nc}^t = \{I_b^{1t}, I_b^{2t}, \dots, \dots, I_b^{NtT}, I_{ab}^{1t}, I_{ab}^{2t}, \dots, \dots, I_{ab}^{NtT}\}. \quad (5)$$

According to some reviews, a model can be built with 50-200 data [37] and to gain a robust YOLOv5 model, that is recommended to train with over 1500 images

per class, and more than 10,000 instances per class [38]. In this study, the target for each class after augmentation is 1500 images for each class. So, the multiplication factor for neutrophil, eosinophil, basophil, lymphocyte, and monocyte is 2.5, 13.8, 8.4, 3.9 and 9.2 respectively. By implementing that multiplication factor, the number of the expected-augmented images for neutrophil, eosinophil, basophil, lymphocyte, and monocyte is 897, 1391, 1321, 1116, and 1337 respectively.

Table 7. Augmentation through Multiplication Factor

No	Class	Image	Multiplication factor	Target	Number of augmented images
0	Neutrophil	603	2.5	1500	897
1	Eosinophil	109	13.8	1500	1391
2	Basophil	179	8.4	1500	1321
3	Lymphocyte	384	3.9	1500	1116
4	Monocyte	163	9.2	1500	1337

After the augmentation is done, the process will generate a lot of data. Absolutely, not all these data can be used to avoid underfitting and overfitting. Therefore, the distribution stage of the augmented result becomes very crucial to prepare this dataset. The results of data augmentation are distributed into 15 different subs by considering the class and the augmentation methods.

The number of augmentation models ( $A_m^g$ ) as in (6) is defined for mentioning several augmentation methods with initialization A1 to A15. The distribution of the augmentation result is proposed to obtain equality with the proportional number of augmented samples ( $N_{pab}$ ).

$$A_m^g = \{A_m^{1g}, A_m^{2g}, \dots, A_m^{ng}\}, \quad (6)$$

$$N_{pab} = \frac{(N_{ET} - N_t)}{A_m^g}. \quad (7)$$



Figure 22. Prepared Augmented Images

Table 8. Distribution of Augmented Images

No	Augmentation	Neutrophil	Eosinophil	Basophil	Lymphocyte	Monocyte
A1	R	299	93	89	372	90
A2	HF-R	299	93	88	372	89
A3	HF	299	93	88	372	90
A4	T-HF-R		93	88		89
A5	T-HF		93	88		89
A6	T-R		93	88		89
A7	T		93	88		89
A8	RZ-HF-R		93	88		89
A9	RZ-HF		93	88		89
A10	RZ-R		93	88		89
A11	RZ-T-HF-R	93	88		89	
A12	RZ-T-HF		92	88		89



A13	RZ-T-R		92	88		89
A14	RZ-T		92	88		89
A15	RZ		92	88		89
Total		897	1391	1321	1116	1337

#### 4.3.1. Image Enhancement-based

The selection of this type of image enhancement-based augmentation is done to re-examine the model development capabilities. In addition to increasing the accuracy of the previous model, this augmentation is based on problems that are often experienced in the data collection process. The problems are contrast, brightness, motion blur, disk blur and noise.

First, the contrast needs to be adjusted properly when observing objects using a microscope. Second, it is very important to adjust the lighting to be able to get good quality observations, because there is a lighting control panel on the microscope. Third, motion blur arises when the operation of the microscope is carried out to scan the object thoroughly. The image capturing process is done by observing as much area of the object as possible by rotating the slide panels both horizontally and vertically on the microscope. Fourth, blur noise is imitated from the focus setting process where when the object is observed, the focus setting needs to be considered to get clear results. Fifth, noise is a representation of the condition of the object which has many other particles or traces resulting from the blood sample preparation process. Those cases can prevent the main object (WBC) to be observed from being observed clearly and in detail.

Initially, the WBC subtypes ( $I_b^t$ ) are selected with several images ( $N_t$ ) as in (2). The number of datasets in each class ( $N_t$ ) is estimated with the augmented target ( $N_{EAT}$ ) to determine the augmentation methods ( $A_b^t$ ) as in (8). The augmentation process is carried out until it reaches the expected target number. This procedure is adopted for selected subtypes of WBC to determine the set of augmentation

method ( $A_b$ ) which describes the number of enhanced images that is produced from each image (n) of a particular subtype of WBC.

. Let  $Ii(x, y)$  be the color value of the  $I^{th}$  channel at position  $(x, y)$  in the image. The first procedure is contrast adjustment ( $C^n$ ) to the image  $Ii(x, y)$  as in (8). The second augmentation is adding gaussian noise  $N$  with mean  $\mu$  and variance  $\sigma^2$  as in (9). Increasing brightness is proposed in this study by adding brightness value  $B^n$  as in (10). The next augmentation is imitated from the acquisition process using microscope by adding certain blur value with motion blur  $Mb$  as in (11) and disk blur  $Db$  as in (12),

$$Ii(x, y) = Ii(x, y) + C^n \quad (8)$$

$$Ii(x, y) = Ii(x, y) + N(\mu, \sigma^2) \quad (9)$$

$$Ii(x, y) = Ii(x, y) + B^n \quad (10)$$

$$Ii(x, y) = Ii(x, y) + Mb \quad (11)$$

$$Ii(x, y) = Ii(x, y) + Db \quad (12).$$

The added contrast (C1) with  $imadjust(I, [0 \ 0.7], [0 \ 1])$ , gaussian noise (G) with mean  $\mu = 0.2$  and variance  $\sigma^2 = 0.0007$  with  $imnoise(I, 'gaussian', 0.1, 0.0007)$ , first brightness increase of +30 (B1) with  $I+30$ , motion blur (MB) with  $fspecial('motion', 25, 0)$ , subtracted contrast (C2) with  $imadjust(I, [0.3 \ 1], [0 \ 1])$ , disk blur (DB) with  $fspecial('disk', 10)$ , first brightness reduction by -30 (B2) with  $I+(-30)$ , second brightness increase of +50 (B3) with  $I+50$ , and second brightness reduction of -50 (B4) with  $I+(-50)$  are selected specifically and measured according to the predetermined values to produce an new augmented data ( $I_{nab}^{nt}$ ) image using a single image ( $I_b^{nt}$ ) as in (14). Finally, all augmented images ( $I_{nab}^{nt}$ ) are added up with the original images ( $I_b^t$ ) to produce new datasets from image enhancement ( $I_{NIC}^t$ ) as in (15) with a nearly balanced sample size across the subtypes of WBC,

$$A_b = \left\{ A_b^t = \left| 1 - \frac{N_t}{N_{EAT}} \right|, t \in [1, 2, \dots, T], N_t < N_{EAT}, \right. \quad (13)$$

$$I_{nab}^{nt} = \{H(I_b^{nt}, C1_a, G_a, B1_a, B1_a, MB_a, C2_a, DB_a, B2_a, B3_a) \mid a \in [1, 2, \dots, A_b^t]\} \quad (14)$$

$$I_{NIC}^t = \{I_b^{1t}, I_b^{2t}, \dots, I_b^{NItT}, I_{nab}^{1t}, I_{nab}^{2t}, \dots, I_{nab}^{NItT}\}. \quad (15)$$

Based on the research of the six models that have been built, it shows that the YOLOv5l model has the most suitable architecture for the detection and counting subtypes of WBC models. The number of datasets that reached 1500 was not the main factor to produce better accuracy. Therefore, the model development at this stage uses an image enhancement-based augmentation dataset with a total target dataset of 1000 images per class.

The number of augmentation methods for neutrophil, eosinophil, basophil, lymphocyte, and monocyte is 0.7, 8.2, 4.6, 1.6, and 5.1 respectively. By achieving the total target, the number of the expected-augmented images for neutrophil, eosinophil, basophil, lymphocyte, and monocyte is 397, 891, 821, 616, and 837 respectively. Thus, the number of original datasets and image enhancement-based augmentation results is 1000 images per class where the total dataset is 5000 images. This augmentation result will be utilized for model training with setting by 16 batch size and 600 epochs.

Table 9. An image enhancement-based augmentation dataset

No	Class	Image	Number of		Number of augmented images
			Augmentation Methods	Target	
0	Neutrophil	603	0.7	1000	397
1	Eosinophil	109	8.2	1000	891
2	Basophil	179	4.6	1000	821
3	Lymphocyte	384	1.6	1000	616
4	Monocyte	163	5.1	1000	837

In more detail, the distribution of augmented results is needed to ensure that the data is properly distributed. each augmentation process is carried out to achieve the target dataset. Once the target has been met, adjustments will be made to the augmented data. The neutrophil class was augmented with the least number among the others which was only done once with the first method, which was increased contrast in 397 images. Eosinophils were augmented by nine techniques to reach 891 images. Basophil was augmented five times. Lymphocytes were authenticated twice with increased contrast and the addition of gaussian noise. and finally, Monocyte was augmented six times to reach 837 images.

*Table 10. Distribution of image enhancement-based augmentation dataset*

No	Subtypes	Neutrophil	Eosinophil	Basophil	Lymphocyte	Monocyte
Au1	Contrast+	397	218	358	384	326
Au2	Gaussian noise	0	218	358	232	326
Au3	Brightness +30	0	218	358	0	326
Au4	Motion blur	0	218	358	0	326
Au5	Contrast -	0	218	210	0	326
Au6	Disk blur	0	218	0	0	22
Au7	Brightness -30	0	218	0	0	0
Au8	Brightness +50	0	218	0	0	0
Au9	Brightness -50	0	38	0	0	0
Total		397	891	821	616	837

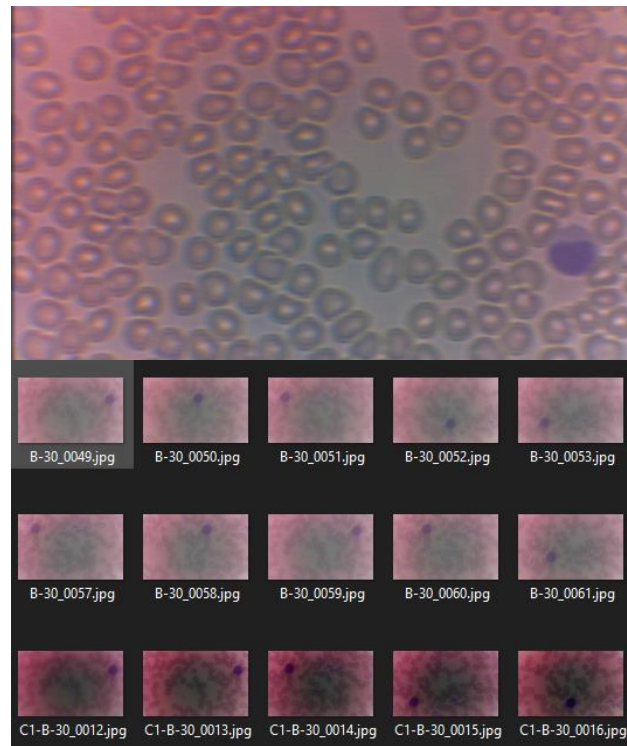


Figure 23 . Image enhancement-based augmentation dataset

### 4.3. Training Result of Raw Data

Preparation to conduct model training with the YOLOv5 model locally requires quite complex steps. In general, the YOLOv5 model is offered to run online through several platforms such as Google Colab or Roboflow. However, considering the amount of data and the length of training time required, and the number of GPU allocations that will be used, training locally is the best choice in developing this model.

Firstly, YOLOv5 needs to be installed via Anaconda Environment. However, before that, the CPU hardware specifications used need to be checked again so that the cloning and installing YOLOv5 process runs properly. One of the challenges for YOLOv5 installation is syncing and installing Pytorch. Developed primarily by Meta AI, PyTorch is an open-source machine learning framework that is based on the Torch library and is used for tasks specifically like computer vision and natural language

processing. To get this support, it is provided online on the PyTorch official website <https://pytorch.org/get-started/locally/>.

### PyTorch Enterprise Support Program.

PyTorch Build	Stable (1.10.1)	Preview (Nightly)	LTS (1.8.2)
Your OS	Linux	Mac	Windows
Package	Conda	Pip	LibTorch
Language	Python	C++ / Java	
Compute Platform	CUDA 10.2	CUDA 11.3	ROCm 4.2 (beta)
Run this Command:	<code>conda install pytorch torchvision torchaudio cudatoolkit=11.3 -c pytorch</code>		

Figure 24. PyTorch Seeting Up

According to the specification of the computer that will be used for training the model, this research selects this specific command. The selected PyTorch Build type is the “Stable (1.10.1) version. based on the operating system used, where the computer used uses the Windows 10 operating system, then the type of OS selected is Windows. This study uses the Anaconda environment so that the package chosen is Conda where the programming language used is python. To have a computer platform, it is chosen based on the specifications of the GPU used which in this case is CUDA 11.3. After all the specifications of the options mentioned above have been selected, the command provided by PyToch will appear to carry out the installation process “*conda install pytorch torchvision torchaudio cudatoolkit=11.3 -c pytorch*”.

**Select Target Platform**

Click on the green buttons that describe your target platform. Only supported platforms will be shown. By downloading and using the software, you agree to fully comply with the terms and conditions of the [CUDA EULA](#).

Operating System: Linux Windows

Architecture: x86\_64




Version: 10 Server 2016 Server 2019

Installer Type: exe (local) exe (network)

Figure 25. CUDA 11.3 Installation

After all stages have been perfectly finished, the training preparation stage is ready to be carried out. The training carried out in this study uses the YOLOv5 model of several types that have differences in performance and network complexity. The models chosen for comparison are YOLOv5s, YOLOv5l, and YOLOv5x. The three models are models with small, large, and extra-large versions which will generate models with different results. The models are built which have different results as mentioned in sub chapter 4.3.1, 4.3.2, and 4.3.3.

Table 11. YOLOv5 Version

Version	Complexity	Size
YOLOv5s (Small Version)	 Small YOLOv5s	90 MB <sub>FP16</sub> 3.8 ms <sub>V100</sub> 48.1 mAP <sub>COCO</sub>
YOLOv5l (Large Version)	 Large YOLOv5l	90 MB <sub>FP16</sub> 3.8 ms <sub>V100</sub> 48.1 mAP <sub>COCO</sub>
YOLOv5x (Extra Large Version)	 XLarge YOLOv5x	168 MB <sub>FP16</sub> 6.0 ms <sub>V100</sub> 50.1 mAP <sub>COCO</sub>

### 4.3.1. YOLOv5s

YOLOv5s is one of YOLOv5 family which has small level of architecture according to the training process and the accuracy. This model is built with 1475 images consisting of 1544 labels which are divided into five different classes which are subtypes of WBC. The model is trained with 600 epochs with 16 batch size. According to the built model, YOLOv5s has 0.995 for mAP@.05 and 0.939 mAP@.5:.95 accuracy.

Class	Images	Labels	P	R	mAP@.5	mAP@.5:.95
all	1475	1544	0.999	1	0.995	0.939
neutrophil	1475	626	0.998	1	0.995	0.949
eosinophil	1475	109	0.999	1	0.995	0.937
basophil	1475	185	1	1	0.995	0.925
lymphocyte	1475	461	1	0.998	0.995	0.944
monocyte	1475	163	1	1	0.995	0.942

Figure 26. YOLOv5s accuracy (Raw Data) with distributed classes

When observed in more detail, the highest accuracy was obtained for neutrophil detection with 0.949 mAP@.5:.95 accuracy. While the lowest accuracy for the detected sub-class is basophil with 0.925 mAP@.5:.95 accuracy. For the other classes, namely eosinophil, lymphocyte and monocyte have 0.937, 0.944 and 0.942 respectively for mAP@.5:.95 accuracy.

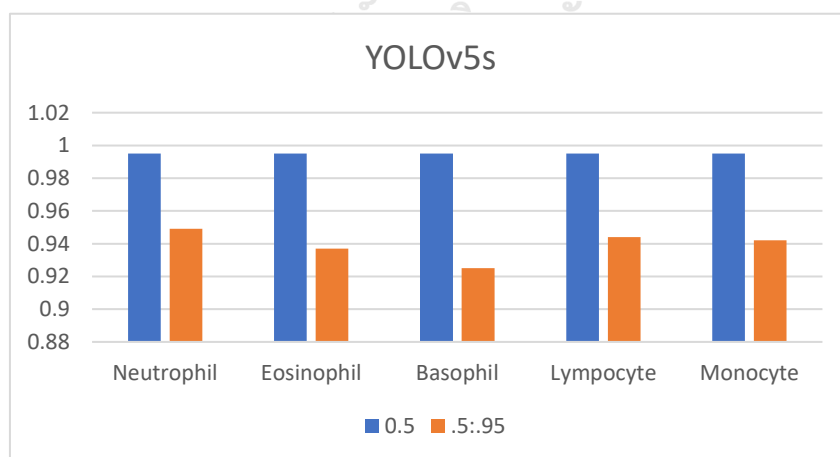


Figure 27. The comparison of YOLOv5s accuracy (Raw Data) for among WBC subtypes



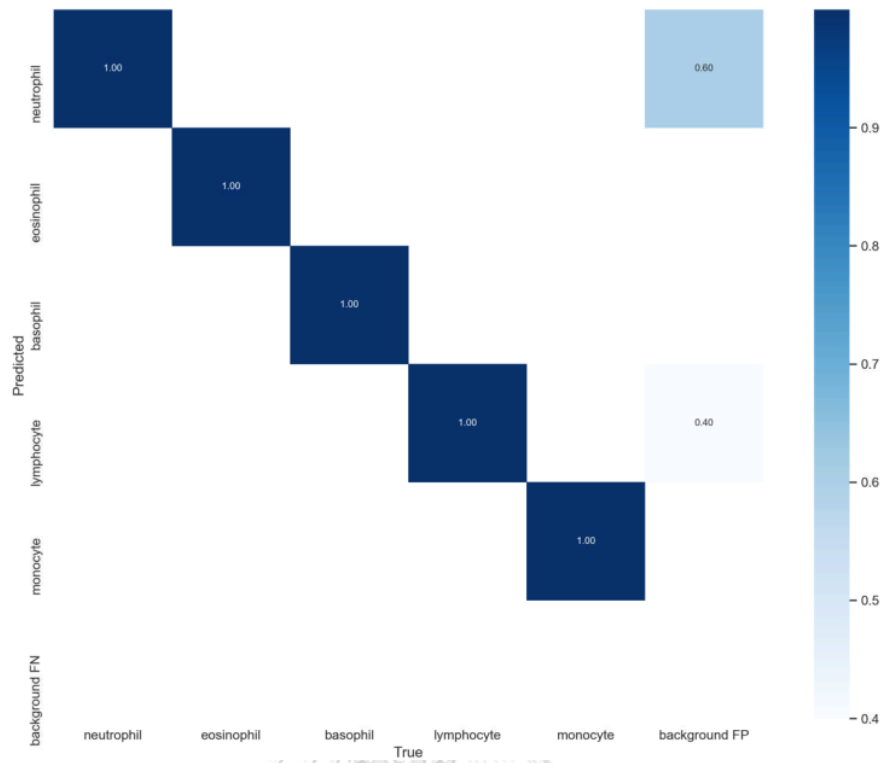


Figure 28. Confusion Matrix YOLOv5s (Raw Data)

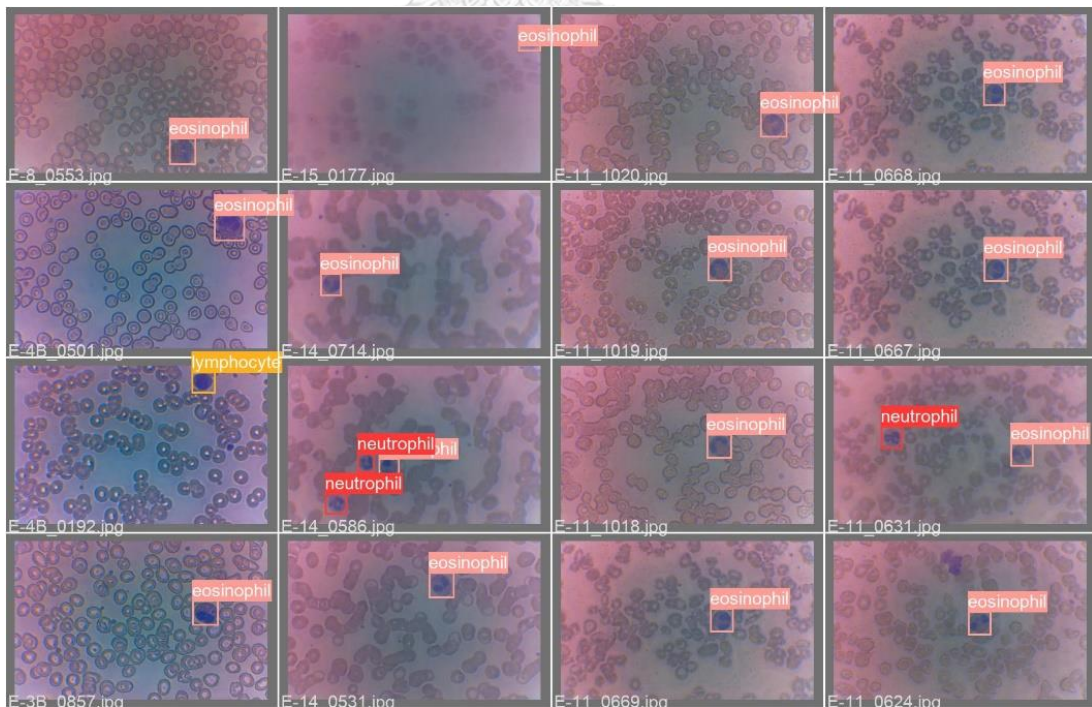


Figure 29. YOLOv5s Prediction (Raw Data)

### 4.3.2. YOLOv5l

YOLOv5l is one of YOLOv5 family which has large performance according to the training process and the accuracy. This model is built with 1475 images consisting of 1544 labels which are divided into five different classes which are subtypes of WBC. The model is trained with 600 epochs and 16 batch size. According to the built model, YOLOv5l has 0.946 mAP@.5:.95 accuracy.

Class	Images	Labels	P	R	mAP@.5	mAP@.5:.95:
all	1475	1544	1	1	0.995	0.946
neutrophil	1475	626	0.998	1	0.995	0.961
eosinophil	1475	109	1	1	0.995	0.945
basophil	1475	185	1	1	0.995	0.937
lymphocyte	1475	461	1	0.998	0.995	0.94
monocyte	1475	163	1	1	0.995	0.946

Figure 30. YOLOv5l accuracy (Raw Data) with distributed classes

When observed in more detail, the highest accuracy was obtained for neutrophil detection with 0.961 mAP@.5:.95 accuracy. While the lowest accuracy for the detected sub-class is basophil with 0.937 mAP@.5:.95 accuracy. For the other classes, namely eosinophil, lymphocyte and monocyte have 0.945, 0.937 and 0.94 respectively for mAP@.5:.95 accuracy.

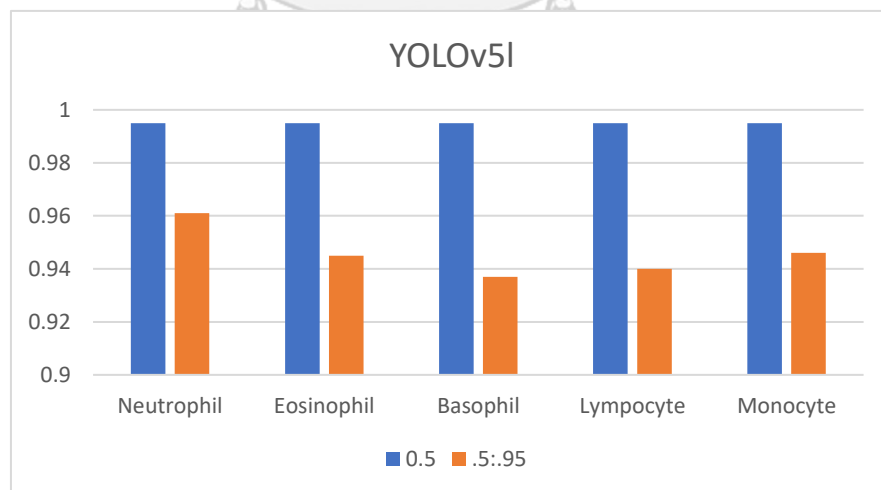


Figure 31. The comparison of YOLOv5l accuracy (Raw Data) for among WBC subtypes

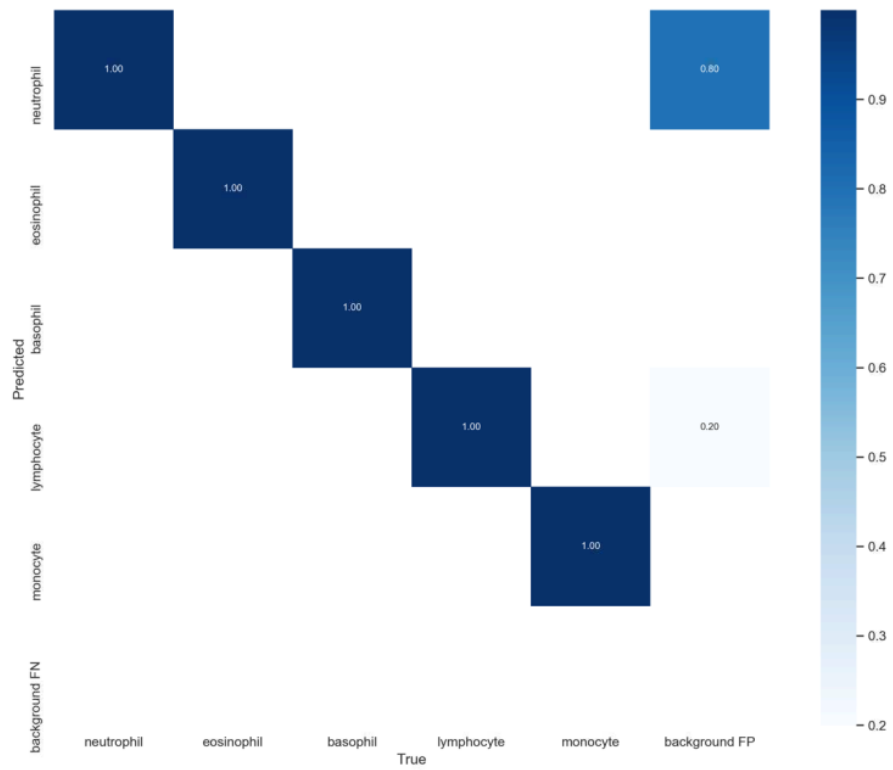


Figure 32. YOLOv5l Confusion Matrix (Raw Data)

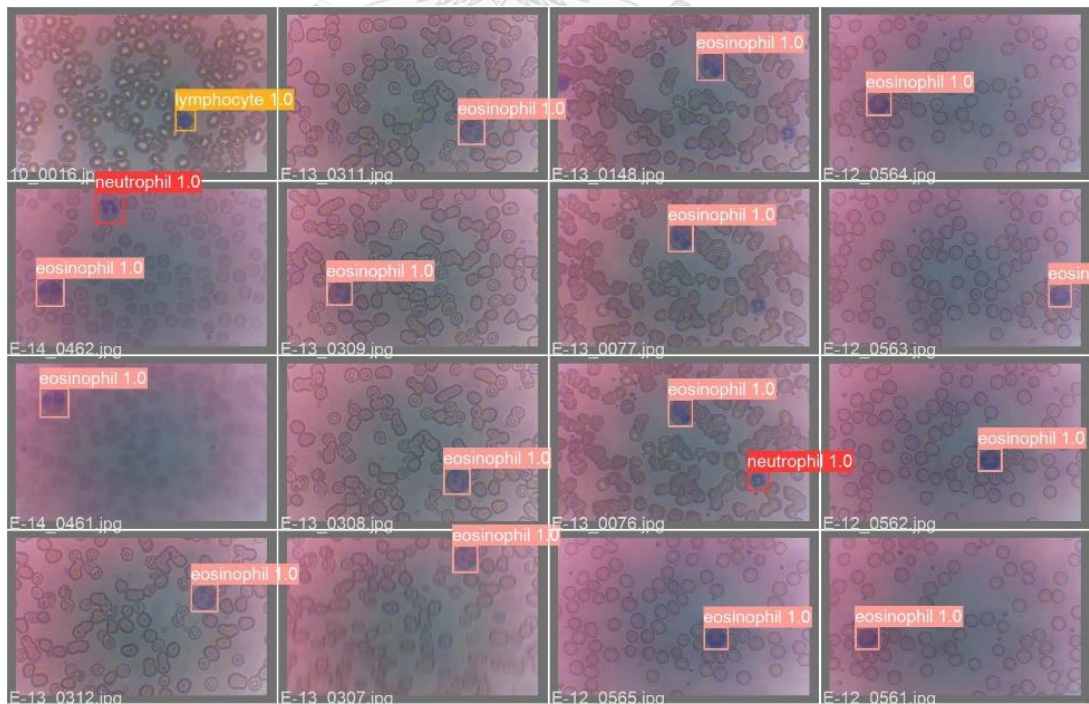


Figure 33. YOLOv5l Prediction (Raw Data)

### 4.3.3. YOLOv5x

YOLOv5x is one of YOLOv5 family which has extra-large performance according to the training process and the accuracy. This model is built with 1475 images consisting of 1544 labels which are divided into five different classes which are subtypes of WBC. The model is trained with 600 epochs and 16 batch size. According to the built model, YOLOv5l has 0.866 mAP@.5:.95 accuracy.

```

Summary: 574 layers, 140009320 parameters, 0 gradients, 208.2 GFLOPs

```

Class	Images	Labels	P	R	mAP@.5	mAP@.5:.95:
all	1475	1544	0.982	0.993	0.994	0.866
neutrophil	1475	626	0.987	0.989	0.994	0.864
eosinophil	1475	109	0.986	1	0.995	0.882
basophil	1475	185	0.977	0.995	0.995	0.888
lymphocyte	1475	461	0.989	0.986	0.994	0.821
monocyte	1475	163	0.97	0.995	0.995	0.874

Figure 34. YOLOv5x accuracy (Raw Data) with distributed classes

When observed in more detail, the highest accuracy was obtained for basophil detection with 0.882 mAP@.5:.95 accuracy. While the lowest accuracy for the detected sub-class is lymphocyte with 0.821 mAP@.5:.95 accuracy. For the other classes, namely neutrophil, eosinophil, and monocyte have 0.864, 0.882 and 0.874 respectively for mAP@.5:.95 accuracy.

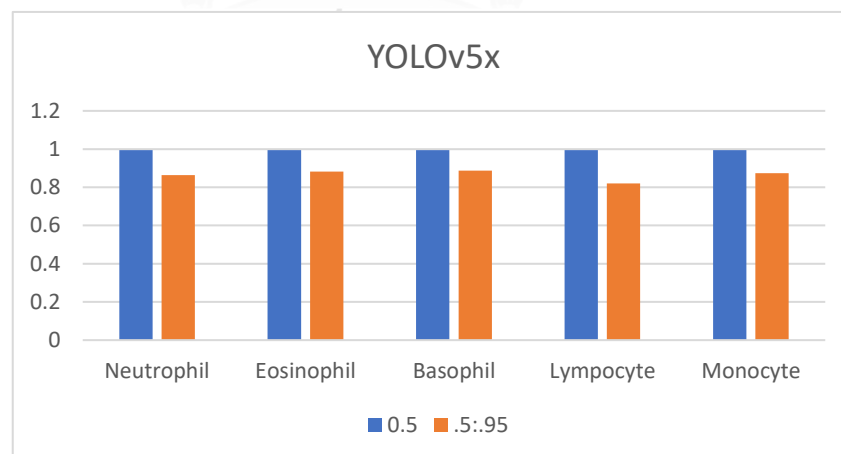


Figure 35. The comparison of YOLOv5x accuracy (Raw Data) for among WBC subtypes

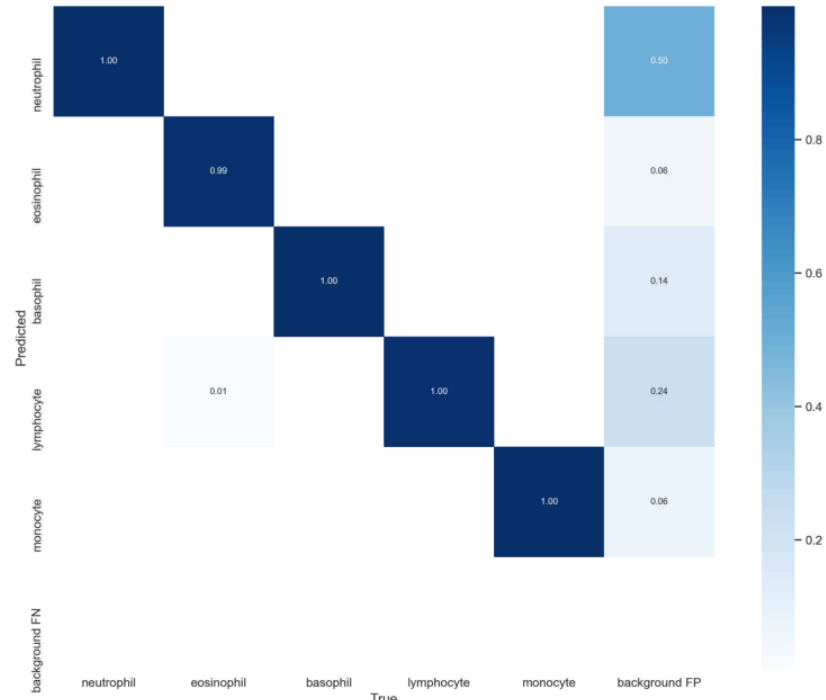


Figure 36. YOLOv5x Confusion Matrix (Raw Data)

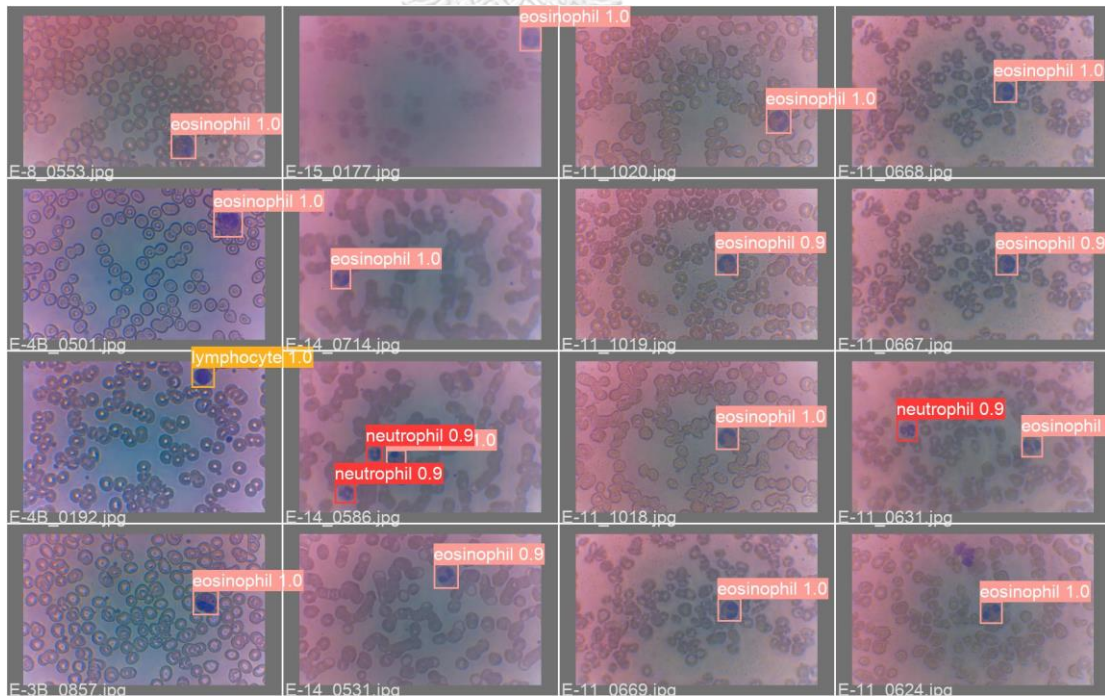


Figure 37. YOLOv5x6 Prediction (Raw Data)

#### 4.4. Training Result of Augmented Data

Data development through the augmentation process aims to enrich the original data to get more variations of the data. The more and varied the data used, the better the model will be built. Before training begins, it is essential to prepare the dataset. The labeling process is a time-consuming process. In this case, the labeling process is carried out semi-automatically using the best model from “Training Result of Raw Data” where the YOLOv5l model that has been built is used to generate labels for a total dataset of 7500 images. So that the labeling process can be completed more quickly.

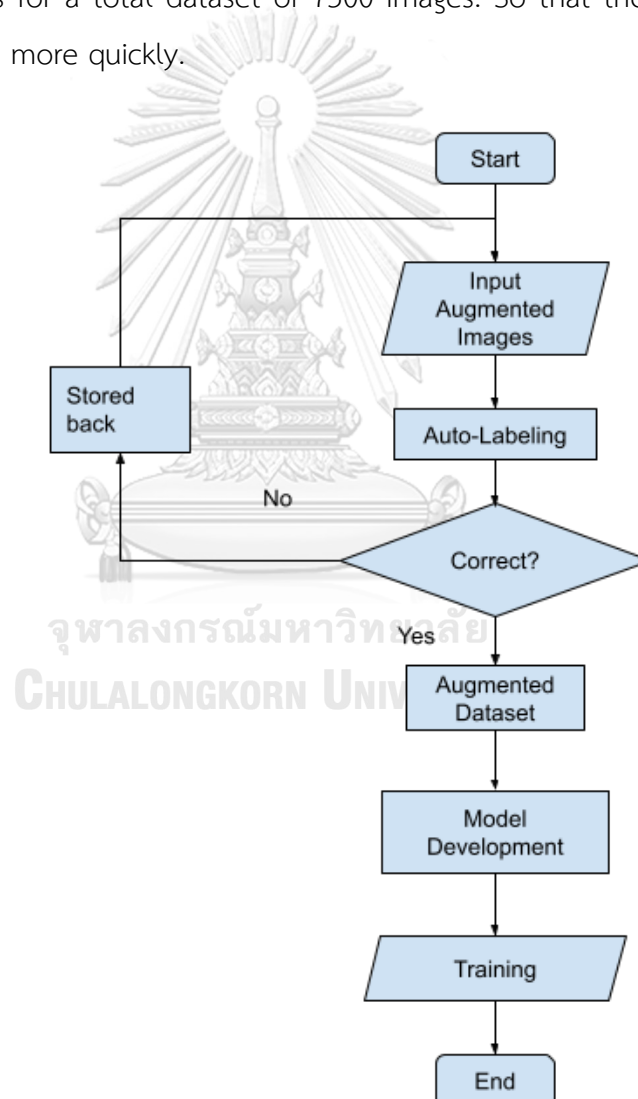


Figure 38. Auto-Labeling

This stage begins with preparing all the augmented images that have been degenerated through several augmentation techniques. The augmentation process uses the parameters written in equation (1) to equation (5). The original dataset can be enriched to be more than 7500 images mathematically. First, from the dataset that has been formed, then labeling is carried out with the auto-labeling technique. All augmented data are used as input for the auto labeling process which will produce bounding boxes and specific classes which are stored in the form of a “.txt” file.

And then, labels will be assigned manually to see the correctness of the data generated from the automatic process. The data that has been confirmed will be designated as a new dataset resulting from the augmentation. Then, the data is compressed until it reaches a composition of 7500 data which is divided into 1500 images for each subtype of WBC. The data is then rearranged for the model development process by considering the composition of the train and test data, where the ratio used is 80:20 for training and testing, respectively.

Simply, the purpose of this augmentation process is to get a balance in the amount of data for each class to be trained. And the semi-automatic labeling process is a way to speed up the process of preparing data with the correct label. Finally, after the data splitting has been prepared, the model training process is ready to begin.

*Table 12. Data Splitting for Augmented Data*

No	Classes	Sample	Train	Test
0	Neutrophil	7500	1200	300
1	Eosinophil	7500	1200	300
2	Basophil	7500	1200	300
3	Lymphocyte	7500	1200	300
4	Monocyte	7500	1200	300

From this augmented data, this study shows the result of training as follow:

#### 4.4.1. YOLOv5s

YOLOv5s is one of YOLOv5 family which has small level of architecture according to the training process and the accuracy. This model is built with 7500 images consisting of 7571 labels which are divided into five different classes which are subtypes of WBC. The model is trained with 600 epochs and 16 batch size. According to the built model, YOLOv5s has 0.971 for mAP@.05 and 0.924 mAP@.5:.95 accuracy.

Class	Images	Labels	P	R	mAP@.5	mAP@.5:.95:
all	7500	7571	0.932	0.987	0.971	0.924
neutrophil	7500	1708	0.982	0.992	0.995	0.944
eosinophil	7500	1471	0.994	0.996	0.995	0.951
basophil	7500	1110	0.741	0.987	0.878	0.846
lymphocyte	7500	1912	0.977	0.976	0.994	0.934
monocyte	7500	1370	0.967	0.985	0.992	0.943

Figure 39. YOLOv5s accuracy (Geometric Operation based) with distributed classes

When observed in more detail, the highest accuracy was obtained for eosinophil detection with 0.951 mAP@.5:.95 accuracy. While the lowest accuracy for the detected sub-class is basophil with 0.846 mAP@.5:.95 accuracy. For the other classes, namely neutrophil, lymphocyte and monocyte have 0.944, 0.934 and 0.943 respectively for mAP@.5:.95 accuracy.

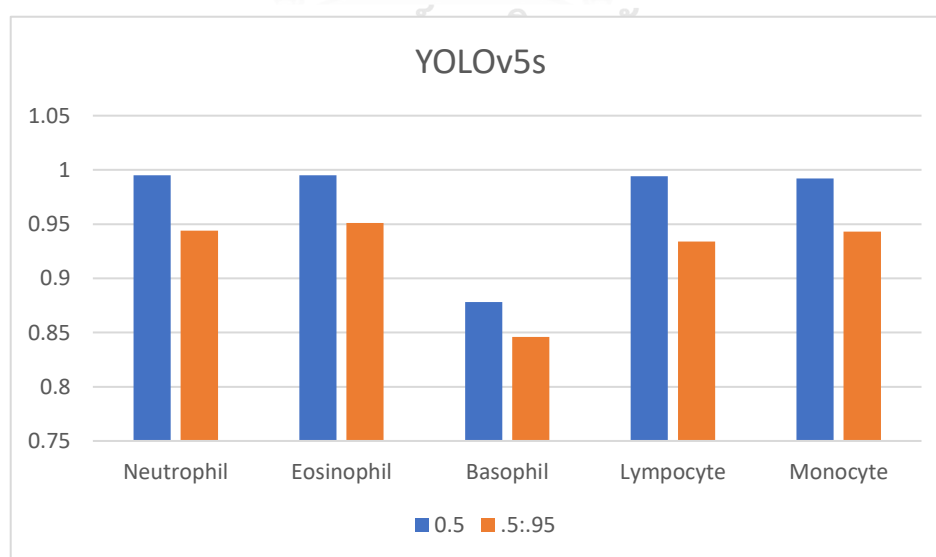


Figure 40. The comparison of YOLOv5s accuracy (Geometric Operation based) for among WBC subtypes



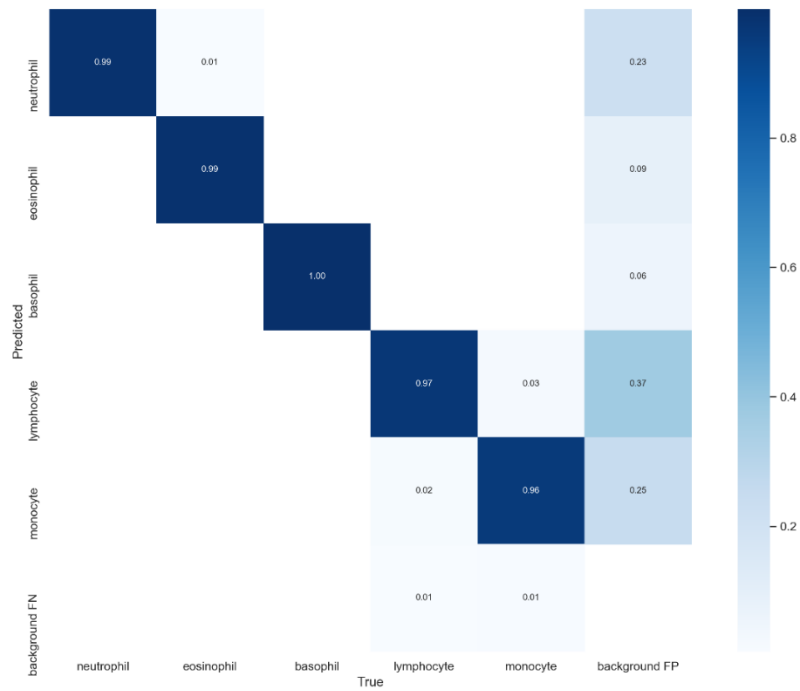


Figure 41. YOLOv5s Confusion Matrix (Geometric Operation based)

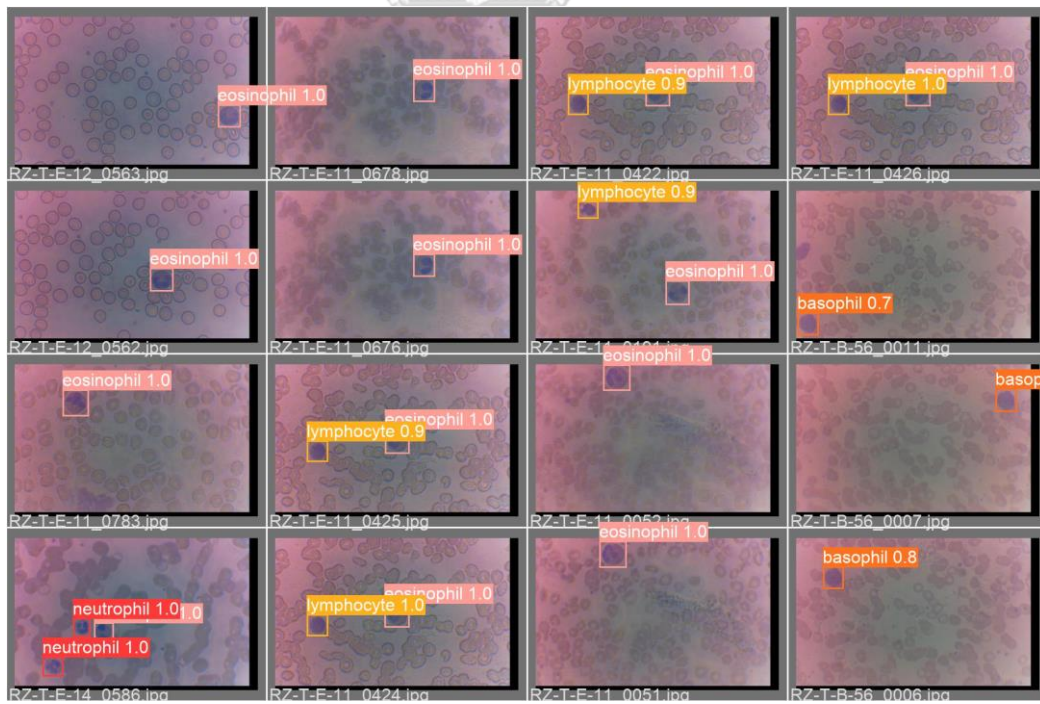


Figure 42. YOLOv5s Prediction (Geometric Operation based)

#### 4.4.2. YOLOv5l

YOLOv5l is one of YOLOv5 family which has large level of architecture according to the training process and the accuracy. This model is built with 7500 images consisting of 7571 labels which are divided into five different classes which are subtypes of WBC. The model is trained with 600 epochs and 16 batch size. According to the built model, YOLOv5s has 0.97 for mAP@.05 and 0.942 mAP@.5:.95 accuracy.

Class	Images	Labels	P	R	mAP@.5	mAP@.5:.95:
all	7500	7571	0.933	0.99	0.97	0.942
neutrophil	7500	1708	0.986	0.992	0.995	0.969
eosinophil	7500	1471	0.995	0.996	0.995	0.973
basophil	7500	1110	0.738	0.994	0.876	0.856
lymphocyte	7500	1912	0.978	0.982	0.994	0.954
monocyte	7500	1370	0.967	0.987	0.989	0.958

Figure 43. YOLOv5l accuracy (Geometric Operation based) with distributed classes

When observed in more detail, the highest accuracy was obtained for eosinophil detection with 0.973 mAP@.5:.95 accuracy. While the lowest accuracy for the detected sub-class is basophil with 0.856 mAP@.5:.95 accuracy. For the other classes, namely neutrophil, lymphocyte and monocyte have 0.969, 0.954 and 0.958 respectively for mAP@.5:.95 accuracy.

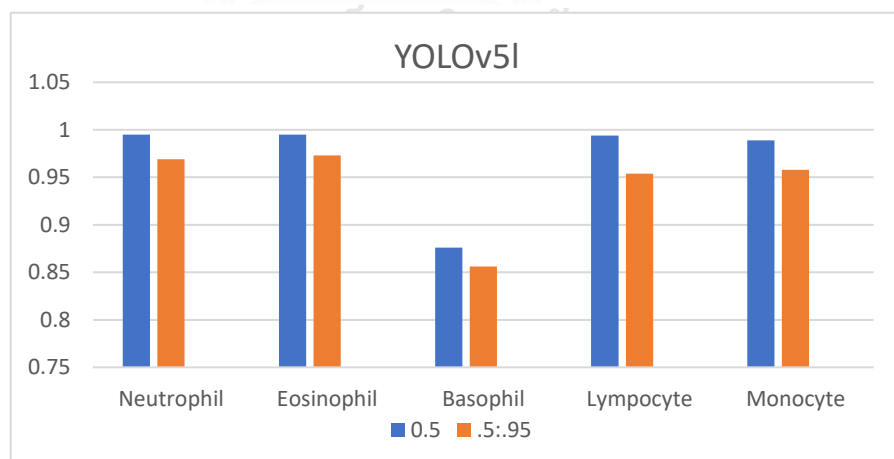


Figure 44. The comparison of YOLOv5l (Geometric Operation based) accuracy for among WBC subtypes

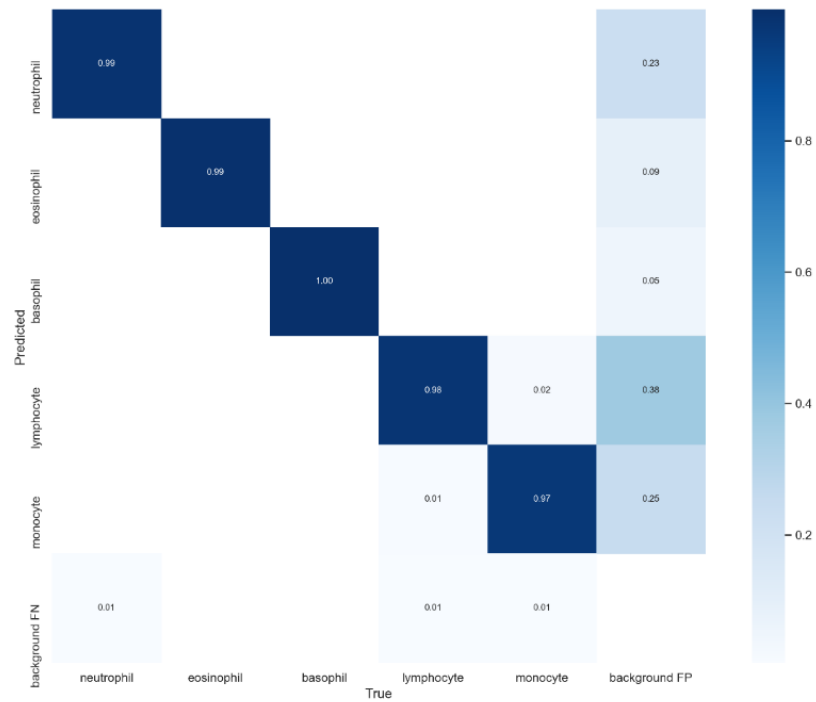


Figure 45. YOLOv5l Confusion Matrix (Geometric Operation based)

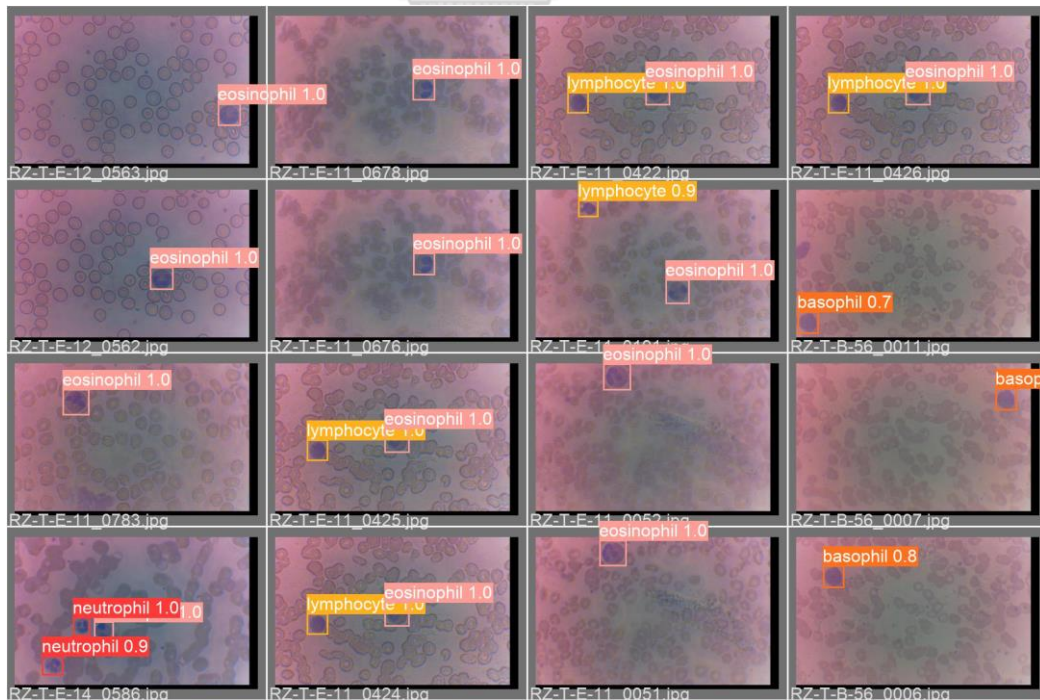


Figure 46. YOLOv5l Prediction (Geometric Operation based)

#### 4.4.3. YOLOv5x

YOLOv5x is one of YOLOv5 family which has extra-large level of architecture according to the training process and the accuracy. This model is built with 7500 images consisting of 7571 labels which are divided into five different classes which are subtypes of WBC. The model is trained with 600 epochs and 16 batch size. According to the built model, YOLOv5s has 0.96 for mAP@.05 and 0.889 mAP@.5:.95 accuracy.

Class	Images	Labels	P	R	mAP@.5	mAP@.5:.95:
all	7500	7571	0.932	0.987	0.96	0.889
neutrophil	7500	1708	0.982	0.99	0.994	0.91
eosinophil	7500	1471	0.993	0.996	0.994	0.947
basophil	7500	1110	0.738	0.986	0.832	0.783
lymphocyte	7500	1912	0.979	0.974	0.993	0.895
monocyte	7500	1370	0.966	0.99	0.989	0.909

Figure 47. YOLOv5x accuracy (Geometric Operation based) with distributed classes

When observed in more detail, the highest accuracy was obtained for eosinophil detection with 0.947 mAP@.5:.95 accuracy. While the lowest accuracy for the detected sub-class is basophil with 0.783 mAP@.5:.95 accuracy. For the other classes, namely neutrophil, lymphocyte and monocyte have 0.91, 0.895 and 0.909 respectively for mAP@.5:.95 accuracy.

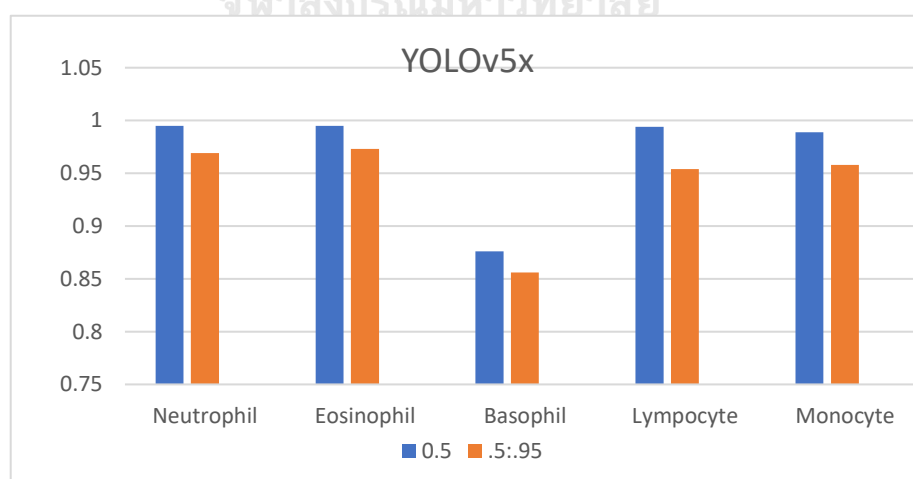


Figure 48. The comparison of YOLOv5x accuracy (Geometric Operation based) for among WBC subtypes

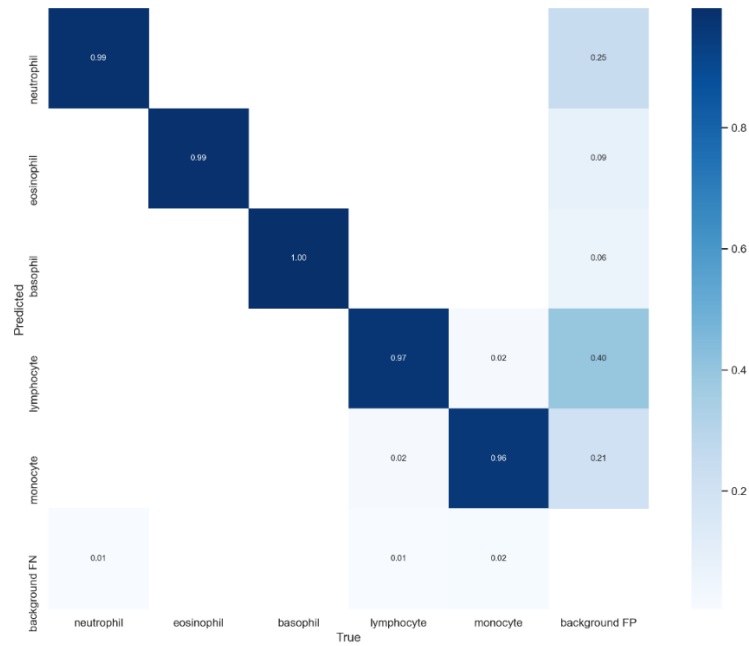


Figure 49. YOLOv5x Confusion Matrix (Geometric Operation based)

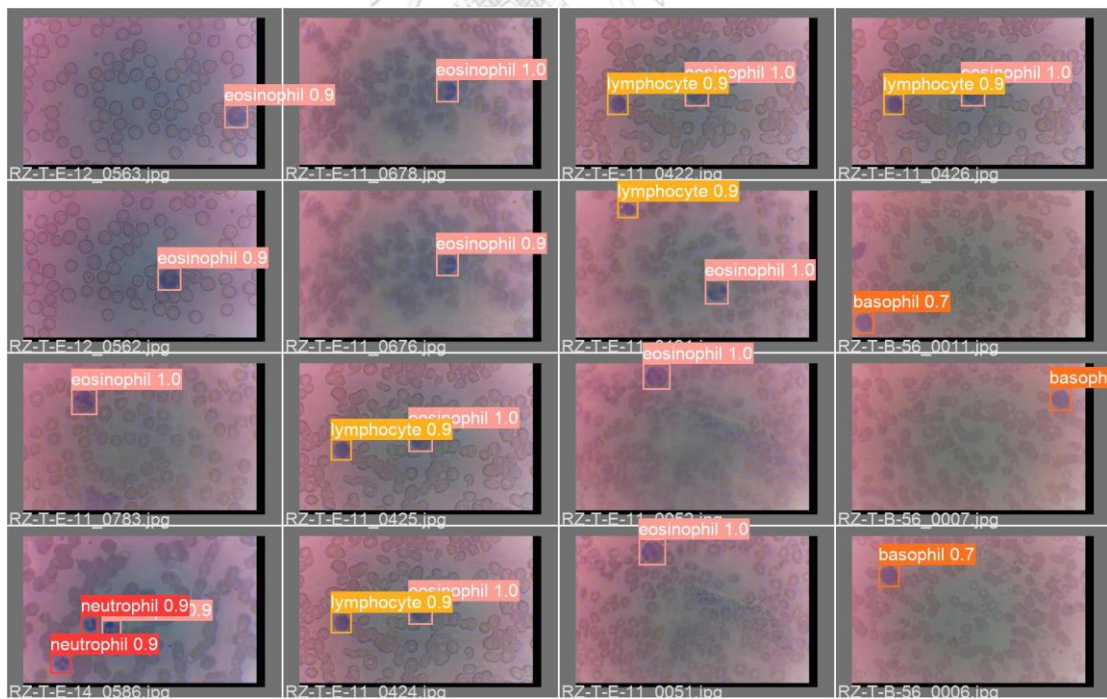


Figure 50. YOLOv5x Prediction (Geometric Operation based)

#### 4.4.4. YOLOv5l image enhancement-based

YOLOv5l is one of YOLOv5 family which has large level of architecture according to the training process and the accuracy. This model is built with 5000 images consisting of 5310 labels which are divided into five different classes which are subtypes of WBC. The model is trained with 600 epochs and 16 batch size. According to the built model, YOLOv5l has 0.995 for mAP@.05 and 0.988 mAP@.5:.95 accuracy.

Class	Images	Labels	P	R	mAP@.5	mAP@.5:.95
all	5000	5310	1	0.999	0.995	0.988
neutrophil	5000	1099	1	1	0.995	0.98
eosinophil	5000	995	1	1	0.995	0.992
basophil	5000	1030	1	1	0.995	0.99
lymphocyte	5000	1188	1	0.997	0.995	0.986
monocyte	5000	998	1	1	0.995	0.994

Figure 51. YOLOv5l accuracy (image enhancement-based data) with distributed classes

When observed in more detail, the highest accuracy was obtained for eosinophil detection with 0.947 mAP@.5:.95 accuracy. While the lowest accuracy for the detected sub-class is basophil with 0.783 mAP@.5:.95 accuracy. For the other classes, namely neutrophil, lymphocyte and monocyte have 0.91, 0.895 and 0.909 respectively for mAP@.5:.95 accuracy.

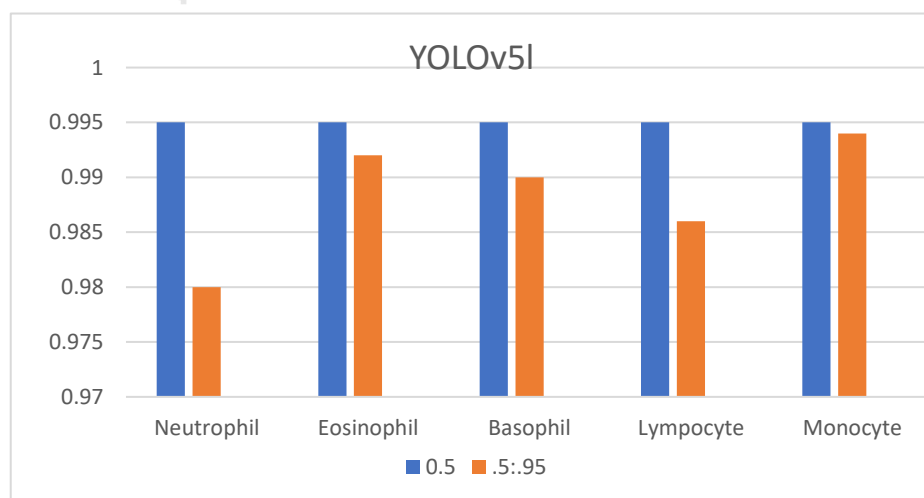


Figure 52. The comparison of YOLOv5l (image enhancement-based data) accuracy for among WBC subtypes

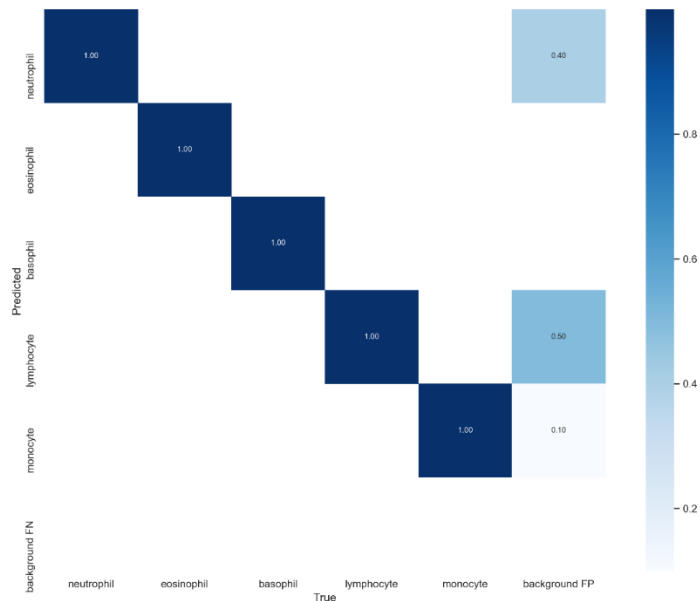


Figure 53. YOLOv5l Confusion Matrix (image enhancement-based data)

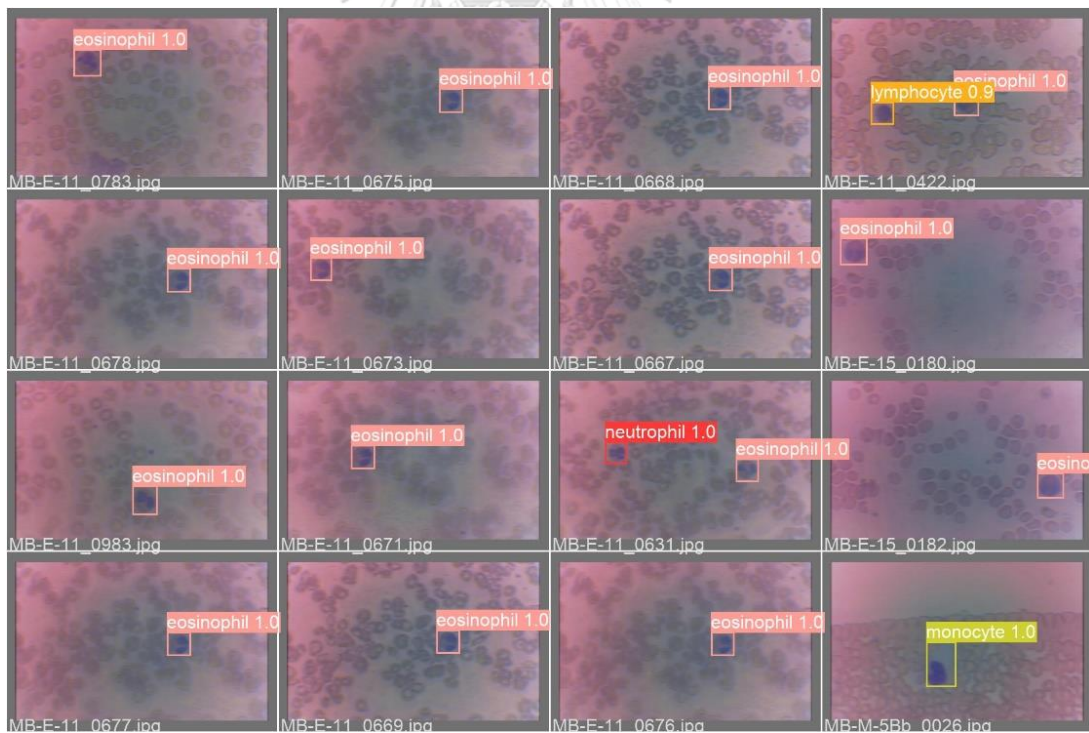


Figure 54. YOLOv5l Prediction (image enhancement-based data)

## 4.5. Comparison of Training Result

### 4.5.1. Geometric Operation

Based on the training results, the first dataset is where raw data is used to build a subtypes of WBC detection model. From the experiment, it shows that the YOLOv5l model has the best performance. The large version model can achieve an accuracy of 0.946 mAP@.5:.95 in 600 epoch and 16 batch size. Then, as an additional option, this experiment shows that YOLOv5s which is a small version of YOLOv5 can achieve an accuracy of 0.937 mAP@.5:.95 with 600 epochs and 16 batch size. Finally, the YOLOv5x model did not provide significant points even though it is with the same batch size and the number epochs for 16 and 600 respectively, the built model is only able to achieve an accuracy of 0.866 mAP@.5:.95.

Table 13. Built Models from Raw Data

Models	mAP.5	mAP.5:.95	Epoch
YOLOv5s	0.995	0.937	600 epochs
YOLOv5l	0.995	0.946	600 epochs
YOLOv5x	0.994	0.866	600 epochs

Data enrichment through augmentation shows different accuracy and performance among three models. Based on training for 7500 images, this study shows that YOLOv5l as the large version of YOLOv5 gains the best performance among others. It obtains 0.942 mAP@.5:.95 accuracy with 600 epoch and 16 batch size. YOLOv5s took longer than YOLOv5x to complete training with 600 epoch and 16 batch size. Meanwhile, the YOLOv5x model is completed with an accuracy of 0.889 and 65,799 for mAP@.5 and mAP@.5:.95 respectively.

Table 14. Built Models from Enrichment Data through Geometric Operation

Models	mAP.5	mAP.5:.95	Epoch
YOLOv5s	0.971	0.924	600 epochs
YOLOv5l	0.97	0.942	600 epochs
YOLOv5x	0.96	0.889	600 epochs



#### 4.5.2. Image Enhancement

The research that has been conducted in point 4.5.1 shows that YOLOv5l is the best candidate in building a detection system with an accuracy of more than 0.94 for mAP.5:.95 for two different types of datasets. The training process using a raw dataset using the YOLOv5l model achieved an accuracy of 0.995 for mAP.5 and an accuracy of 0.946 mAP.5:.95. compared to the other two models, YOLOv5s and YOLOv5x give not much better results.

The complexity of the neural network provided is one of the distinguishing factors. The network complexity provided by YOLOv5s is not suitable for constructing the 5 subtype of WBC detection model in this study. Meanwhile, YOLOv5x with a higher complexity than the other two models, produces accuracy results that are not better than YOLOv5l. Networks that are too complex work less than optimally to build a detection model for the 5 subtypes of WBC in this research.

Therefore, the augmentation test will be carried out again by building a model using the dataset generated from the augmentation process based on image enhancement techniques. The highest accuracy value of the three datasets built was generated by YOLOv5l with the augmentation process based on image enhancement techniques. The accuracy values for mAP.5 are 0.995 and 0.988 for mAP.5:.95. Then, the second highest accuracy is obtained by YOLOv5l which is built from the raw dataset with 0.995 for mAP.5 and 0.946 for mAP.5:.95. Meanwhile, the model with the lowest accuracy is built from the accumulated raw data and augmented data based on geometric operations with an accuracy of 0.971 and 9.942 for mAP.5 and mAP.5:.95 respectively.

Table 15. YOLOv5l in 3 different datasets

Models	mAP.5	mAP.5:.95	Epoch
YOLOv5l (Raw Data)	0.995	0.946	600 epochs
YOLOv5l (Geometric Operation-based)	0.97	0.942	600 epochs
YOLOv5l (Image Enhancement-based)	0.995	0.988	600 epochs

Taking consideration to the time required for training the dataset of the three models, YOLOv5l which was built with limited data where raw data is trained unequally completes the training process of 600 epochs. The longest time for training is required by the YOLOv5l model using geometric operation-based augmentation with 7500 images for 5 classes. Finally, the most ideal time to complete the training of all the built models was obtained by the YOLOv5l model using a dataset of image enhancement-based augmentation.

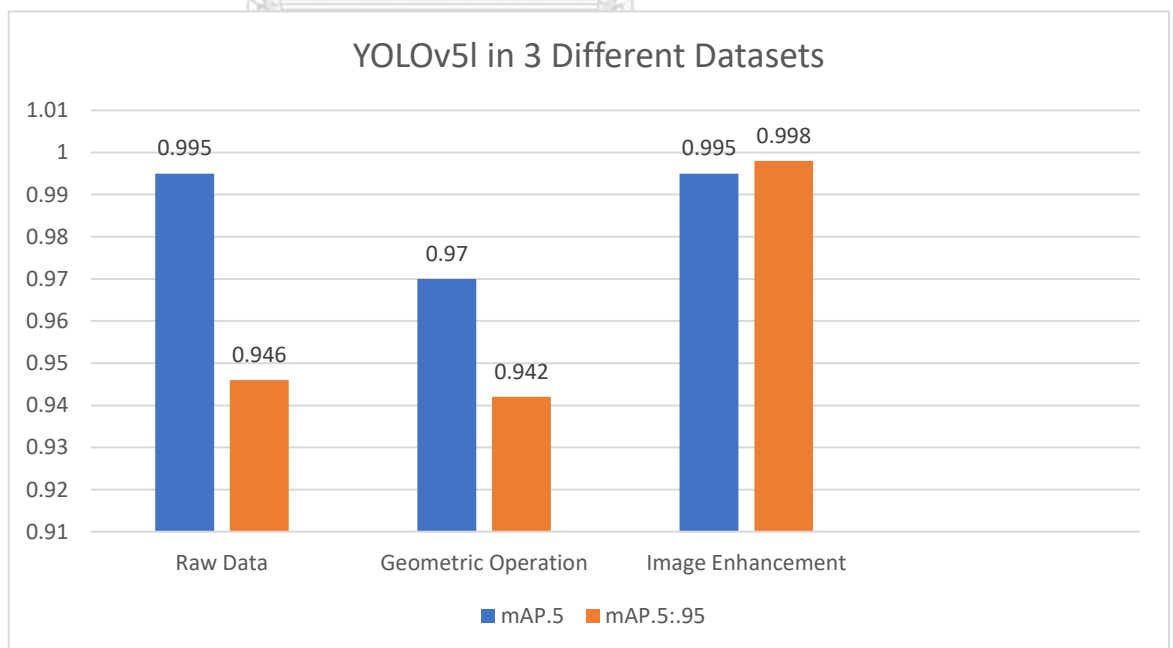
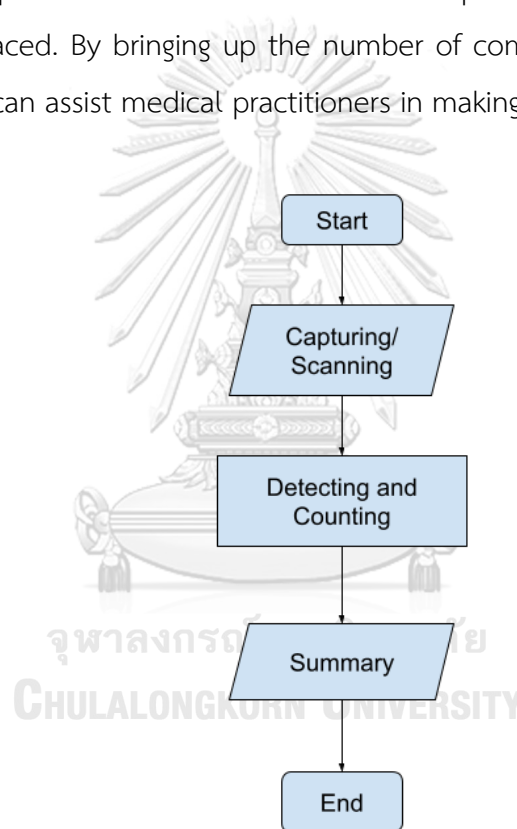


Figure 55. YOLOv5l in 3 Different Datasets

#### 4.6. Blood Counting

Counting the number of subtypes of WBC is an essential part of a Step to find out a diagnosis. This is because the composition of each subtype is not naturally balanced. When the composition changes under certain conditions, it can indicate that the subtypes of WBC are working against something foreign that enters the body. Each of the subtypes of WBC has a different role depending on the conditions and types of threats faced. By bringing up the number of compositions of each subtype of WBC, this step can assist medical practitioners in making further diagnoses.



*Figure 56. Counting Process*

The calculation of WBC subtypes in this study will use sample images taken from the scanning process. This is because WBC generally has a larger size than red blood cells. If the calculation is only based on one frame, the results cannot be correlated more comprehensively. In addition, the WBC color is almost the same for all its subtypes, so it is necessary to adjust the focus on several spots to adjust the

thickness of the object that affects the focus of the observed cells. Moreover, the WBC observation process with a size of 10 is less than the maximum to be able to see the WBC in detail in the shape of the cell. Size 40 is the most ideal size for WBC observations where it is not over in the size, so that the image scanning process can be carried out properly.

The process of detecting and calculating subtypes of WBC will be tested under four conditions, namely:

### 1. Detection Test for Single Cell in Single Image

This test aims to test the ability of the model that has been built to detect and count the number of subtypes of WBC. This test is very similar to the model development process where there is a single cell of WBC in one image. Then a folder containing 100 images consisting of 5 basophils, 5 eosinophils, 20 monocytes, 20 lymphocytes and 51 neutrophils will be analyzed. The folder can represent the name or information of a patient whose blood will be observed.

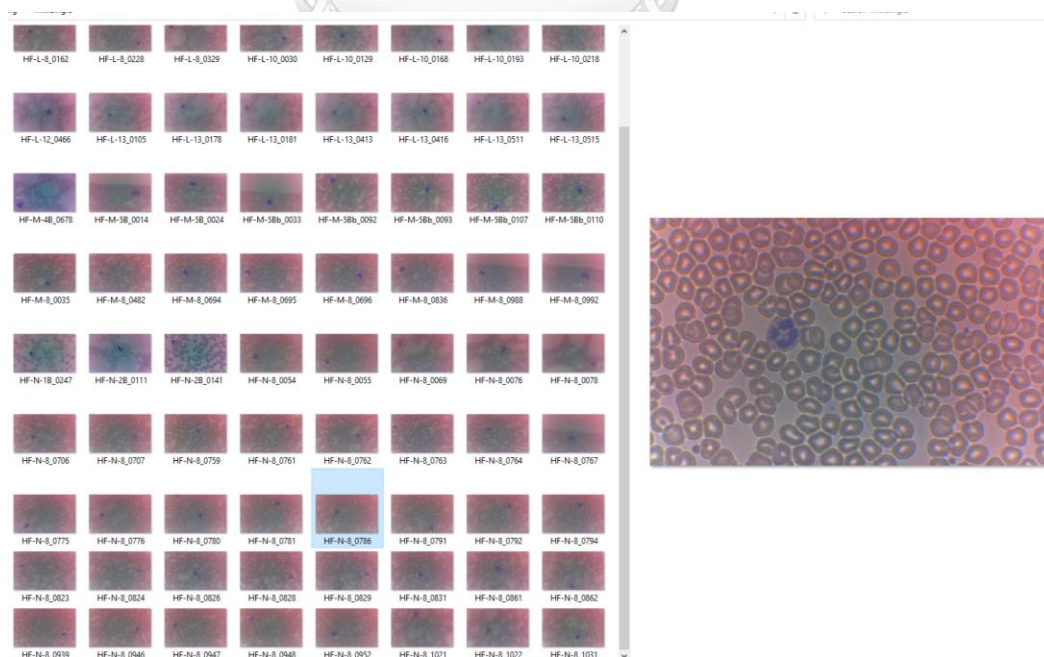
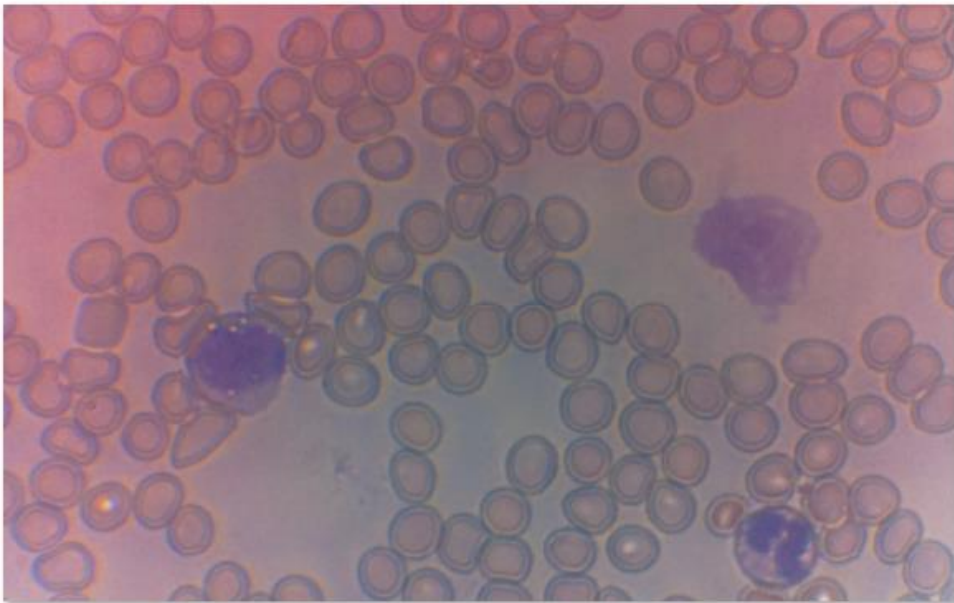


Figure 57. Testing Single Cell in Single Image

## 2. Detection Test for Multiple Cell

At this testing stage, the model that has been built will be tested to detect several WBCs contained in an image. Then, some images which contain different types of WBC will be placed in a folder. Then the model is tested for detection.



*Figure 58. Testing Multiple Cell in Single Image*

## 3. Detection Test for No Cell

In the process of developing the model, this study found that some blood samples did not have WBCs. In some samples, the WBC has been damaged and is not counted as part of the active WBC. In other cases, some samples do not have WBCs due to certain diseases. This test will test the confidential level of the model to interpret samples that do not have WBC completely.

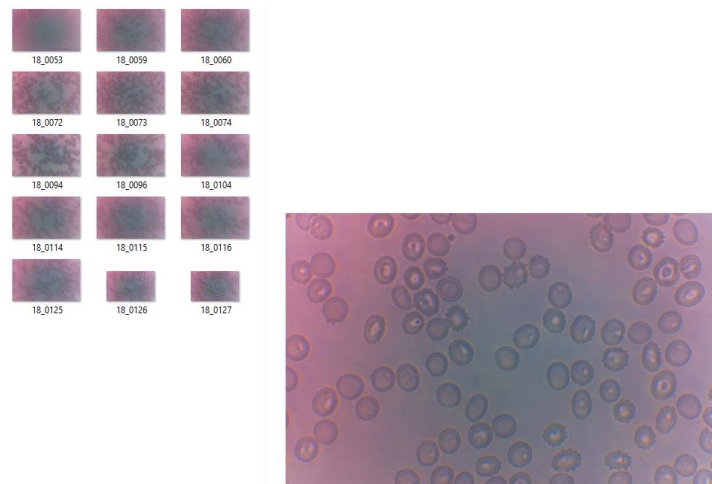


*Figure 59. Testing No Cell in Single Image*

#### 4. Detection Test for Unidentified Subtype

Myelocyte is one type of WBC which is found in the research process. A myelocyte is also called a young cell of the granulocytic series, it is occurring normally in bone marrow. Myelocyte can be found in circulating blood when caused by certain diseases. However, this study did not identify this subtype. The shape and color of this subtype is similar with that of monocytes and some conditions resemble others. This test aims to test how far the myelocyte can be identified by the machine.

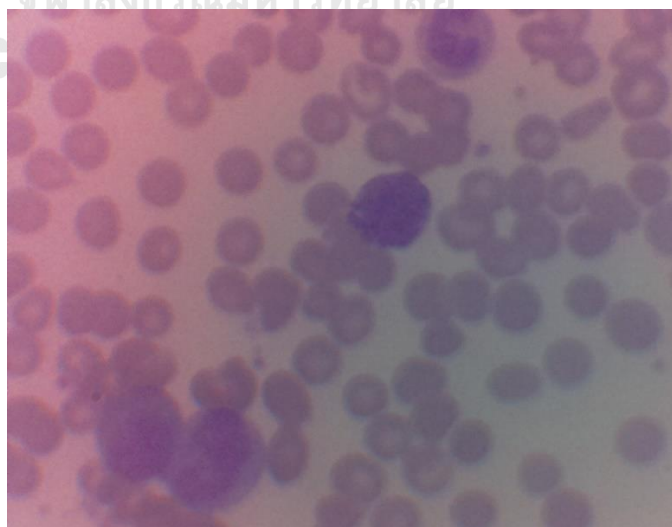


*Figure 60. Testing Unidentified Cell*

#### 4.6.1. YOLOv5 Counting (Raw Data Model)

The first detection and calculation test apply the YOLOv5s, YOLOv5l and YOLOv5x models which are built using raw data. The results of this test show good results where the detection and calculation results are perfect. The number of neutrophils counted was 51 of the totals presented 50 images with one additional neutrophil present in the same frame as the lymphocyte.

Table 16. Detection and Counting Using Model in Single Cell in an Image

No	Class	Correct	YOLOv5s	YOLOv5l	YOLOv5x
0	Neutrophil	51	51	51	51
1	Eosinophil	5	5	5	5
2	Basophil	5	5	5	5
3	Lymphocyte	20	20	20	22
4	Monocyte	20	20	20	20

The table above explains that to detect and count neutrophils, eosinophils, basophils, and monocytes, the three models have the same performance. Meanwhile, YOLOv5x has an error in detecting lymphocytes where there are 22 lymphocytes detected from the number of 20 cells prepared.

The detection results are presented in the form of data for each class in a file with \*.xlsx format. These results can also be interpreted in the form of a pie chart to describe the composition of each subtype of WBC.

HF-N-8_0947.txt	0	0.184028	0.432222	0.0986111	0.16
HF-N-8_0948.txt	0	0.197222	0.272778	0.0930556	0.147778
HF-N-8_0952.txt	0	0.305556	0.656667	0.113889	0.18
HF-N-8_1021.txt	0	0.392014	0.155556	0.107639	0.195556
HF-N-8_1022.txt	0	0.35	0.583889	0.108333	0.192222
HF-N-8_1031.txt	0	0.573264	0.744444	0.103472	0.168889
Neutrophil	51				
Eosinophil	5				
Basophil	5				
Lymphocyte	20				
Monocyte	20				

Figure 61. Counting Result of YOLOv5s Model (Raw Data)

From the results of the calculations that have been carried out, these results can be summarized into statistical data to be read more easily and quickly. In percent units, neutrophil, eosinophil, basophil, lymphocyte, and monocyte are 50%, 5%, 5%, 20% and 20% respectively.

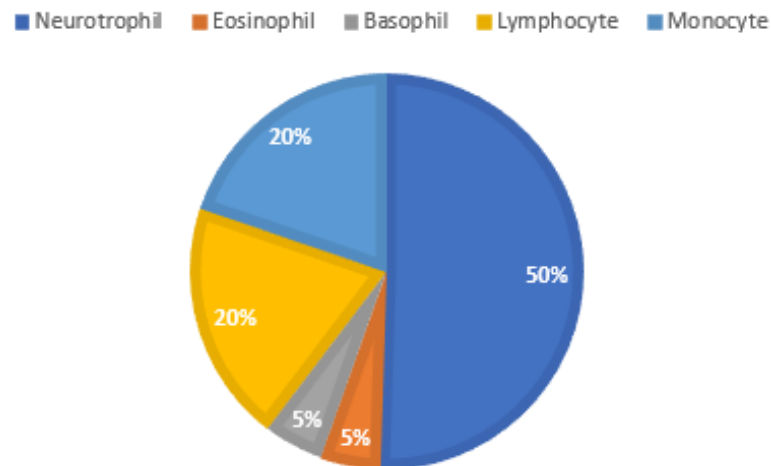


Figure 62. Chart of Counting Result of YOLOv5s (Raw Data)

The second calculation test is to calculate the different subtypes in one frame. In the neutrophil class, of the 17 cells that should be detected, only 11 cells can be detected. Detection for eosinophils and basophils was flawless, detecting only 1 cell for each of the two. Lymphocytes account for 3 out of 4 in the data. And finally, monocytes detected 4 cells out of a total of 3 cells that were available in the data.

Table 17. Detection and Counting from Built Model based on the Raw Data in Multiple Cell in an Image

No	Class	Correct	YOLOv5s	YOLOv5l	YOLOv5x
0	Neutrophil	17	11	11	13
1	Eosinophil	1	1	1	1
2	Basophil	1	1	1	1
3	Lymphocyte	4	3	4	4
4	Monocyte	3	4	2	3

Furthermore, the counting results from the YOLOv5l model have a performance that is not much different from that of YOLOv5s. Its detection ability is



slightly off the mark in detecting 2 monocytes, which are counted from a total of 3 cells. And lastly, YOLOv5x has a satisfactory performance by being able to detect more neutrophils than the two previous models. This model is able to detect 13 neutrophils out of a total of 17 cells. And for other subtypes can be detected correctly.

HF-E-11_0423.txt	3	0.791319	0.599444	0.0840278	0.143333
HF-E-11_0423.txt	1	0.464583	0.534444	0.1	0.162222
RZ-B-59_0235.txt	2	0.129722	0.556444	0.115	0.184889
Neutrophil	13				
Eosinophil	1				
Basophil	1				
Lymphocyte	4				
Monocyte	3				

Figure 63. Counted Cell of YOLOv5x (Raw Data)

The third trial shows that the three models have the same performance where none of the WBCs is detected from a total of 0 WBCs and only red blood cells were provided. And the last test is to try to detect myelocytes which are undefined subtypes of WBC in this study. There are 5 basophils in 5 images where each image has myelocytes. From the results of calculations performed, the three models have the same ability not to identify myelocytes into the model.

Table 18. Detection and Counting from Built Model based on Raw Data on Unidentified Cell in an Image

No	Class	Correct	YOLOv5s	YOLOv5l	YOLOv5x
0	Neutrophil	0	0	0	0
1	Eosinophil	0	0	0	0
2	Basophil	5	5	5	5
3	Lymphocyte	0	0	0	0
4	Monocyte	0	0	0	0

#### 4.6.2. YOLOv5 Counting (Augmented Data Model)

The next detection and calculation test apply the YOLOv5s, YOLOv5l and YOLOv5x models which are built using augmented data. The results of this test show perfect results where the detection and calculation results are remarkable. The number of neutrophils counted was 51 of the totals presented 50 images with one additional neutrophil present in the same frame as the lymphocyte.

*Table 19. Detection and Counting from Built Model based on Geometric Operation Augmentation-based in Single Cell in an Image*

No	Class	Correct	YOLOv5s	YOLOv5l	YOLOv5x
0	Neutrophil	51	51	51	51
1	Eosinophil	5	5	5	5
2	Basophil	5	4	5	5
3	Lymphocyte	20	20	20	19
4	Monocyte	20	20	20	20

The table above explains that to detect and count neutrophils, eosinophils, basophils, and monocytes, the three models have the same performance. Meanwhile, YOLOv5s has an error in detecting basophil where there are 4 basophils detected from the total number of 5 cells prepared. And YOLOv5x detects only 19 lymphocytes from the number of 20 cells prepared. The best model from this dataset in this testing is YOLOv5l which can detect and count perfectly.

The detection results from YOLOv5l are presented in the form of data for each class in a file with \*.xlsx format. These results can also be interpreted in the form of a pie chart to describe the composition of each subtype of WBC.

HF-N-8_0948.txt	0	0.196875	0.272778	0.0951389	0.154444
HF-N-8_0952.txt	0	0.305556	0.657222	0.1125	0.174444
HF-N-8_1021.txt	0	0.393403	0.156111	0.109028	0.192222
HF-N-8_1022.txt	0	0.351736	0.585	0.107639	0.187778
HF-N-8_1031.txt	0	0.573611	0.746111	0.105556	0.165556
Neutrophil	51				
Eosinophil	5				
Basophil	5				
Lymphocyte	20				
Monocyte	20				

Figure 64. Counting Result of YOLOv5l (Geometric Operation based)

From the results of the calculations that have been carried out, these results can be summarized into statistical data to be read more easily and quickly. In percent units, neutrophil, eosinophil, basophil, lymphocyte, and monocyte are 50%, 5%, 5%, 20% and 20% respectively.

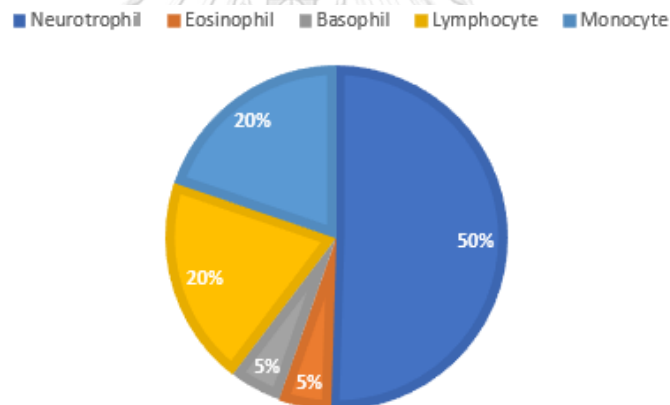


Figure 65. Chart of Counting Result of YOLOv5l (Geometric Operation based)

The second calculation test is to calculate the different subtypes in one frame. In the neutrophil class, YOLOv5s detects 11 cells from the 17 cells that are prepared. Detection for eosinophils and basophils is flawless, detecting only 1 cell for each of the two. Lymphocytes account for 3 out of 4 in the data. And finally, monocytes detected 2 cells out of a total of 3 cells that were available in the data. YOLOv5l detects correctly only for eosinophil. And YOLOv5x detects more neutrophil among others with missing detection only for lymphocyte where 3 cells are detected from 4 cells prepared.

Table 20. Detection and Counting of Built Model with Geometric Operation Augmentation-based for Multiple Cell in an Image

No	Class	Correct	YOLOv5s	YOLOv5l	YOLOv5x
0	Neutrophil	17	11	10	12
1	Eosinophil	1	1	1	1
2	Basophil	1	1	0	1
3	Lymphocyte	4	3	5	3
4	Monocyte	3	2	2	3

Furthermore, the counting results from the YOLOv5l model have a performance that is not much different from that of YOLOv5s. Its detection ability is slightly off the mark in detecting 2 monocytes, which are counted from a total of 3 cells. And lastly, YOLOv5x has a satisfactory performance by being able to detect more neutrophils than the two previous models. This model is able to detect 13 neutrophils out of a total of 17 cells. And for other subtypes can be detected correctly.

HF-E-11_0423.txt	3	0.791319	0.6	0.0854167	0.142222
HF-E-11_0423.txt	1	0.463889	0.535	0.101389	0.158889
RZ-B-59_0235.txt	2	0.130278	0.554667	0.112778	0.183111
Neutrophil	12				
Eosinophil	1				
Basophil	1				
Lymphocyte	3				
Monocyte	3				

Figure 66. Counted Cell of YOLOv5x (Geometric Operation)

The third trial shows that the three models have the same performance where none of the WBCs is detected from a total of 0 WBCs and only red blood cells were provided. And the last test is to try to detect myelocytes which are undefined subtypes of WBC in this study. There are 5 basophils in 5 images where each image has myelocytes. From the results of calculations performed, the three models have the same ability not to identify myelocytes into the model. However, YOLOv5x in this case cannot detect one basophil which is prepared to be analyzed.

*Table 21. Detection and Counting of Built Model with Geometric Operation Augmentation-based for Multiple Cell in Multiple Cell in an Image*

No	Class	Correct	YOLOv5s	YOLOv5l	YOLOv5x
0	Neutrophil	0	0	0	0
1	Eosinophil	0	0	0	0
2	Basophil	5	5	5	4
3	Lymphocyte	0	0	0	0
4	Monocyte	0	0	0	0

#### 4.6.1. YOLOv5l Counting (Image Enhancement-based))

The last detection and calculation test apply the YOLOv5l model which is built using augmented data using image enhancement based. The results of this test show good results where the detection and calculation results are perfect. The number of neutrophils counted is 51 of the totals presented 51 images with one additional neutrophil present in the same frame as the lymphocyte.

*Table 22. Detection and Counting of Built Model with Image Enhancement Augmentation-based for Single Cell in an Image*

No	Class	Correct	YOLOv5l
0	Neutrophil	51	51
1	Eosinophil	5	5
2	Basophil	5	5
3	Lymphocyte	20	20
4	Monocyte	20	20

The table above explains that to detect and count neutrophils, eosinophils, basophils, and monocytes, the YOLOv5l model has the remarkable performance for all subtypes detection. Eosinophil and basophil are detected perfectly 5 cells from 5

cells provided. Additionally, lymphocyte and monocyte are counted precisely 20 cells from 20 cells prepared.

HF-N-8_0952.txt	0	0.304861	0.656667	0.113889	0.175556
HF-N-8_1021.txt	0	0.393403	0.155	0.109028	0.192222
HF-N-8_1022.txt	0	0.35	0.584444	0.109722	0.191111
HF-N-8_1031.txt	0	0.572917	0.745	0.104167	0.165556
Neutrophil	51				
Eosinophil	5				
Basophil	5				
Lymphocyte	20				
Monocyte	20				

Figure 67. Counting Result of YOLOv5l using Augmentation (Image Enhancement-based)

From the results of the calculations that have been carried out, these results can be summarized into statistical data to be read more easily and quickly. In percent units, neutrophil, eosinophil, basophil, lymphocyte, and monocyte are 50%, 5%, 5%, 20% and 20% respectively.

■ Neutrophil ■ Eosinophil ■ Basophil ■ Lymphocyte ■ Monocyte

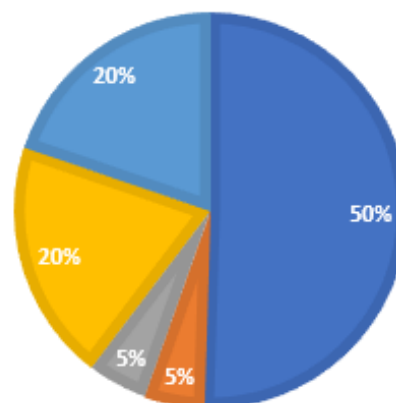


Figure 68. Chart of Counting Result of YOLOv5s (Image Enhancement)

The second calculation test is to calculate the different subtypes in one frame. In the neutrophil class, of the 17 cells that should be detected, only 11 cells can be detected. Detection for eosinophils and basophils is flawless, detecting only 1 cell for each of the two. And finally, lymphocyte and monocytes are completely

detected for 4 and 3 cells respectively out of a total of 4 and 3 cells respectively that are available in the prepared test data.

*Table 23. Detection and Counting of Built Model with Image Enhancement Augmentation-based for Multiple Cell in an Image*

No	Class	Correct	YOLOv5l
0	Neutrophil	17	11
1	Eosinophil	1	1
2	Basophil	1	1
3	Lymphocyte	4	4
4	Monocyte	3	3

Furthermore, the counting results from the YOLOv5l model have a performance that is not much different from that of YOLOv5s in previous discussion.

B_0335.txt	4	0.791319	0.421111	0.150694	0.235556
HF-E-11_0423.txt	3	0.790972	0.597222	0.0847222	0.141111
HF-E-11_0423.txt	1	0.465625	0.534444	0.100694	0.16
RZ-B-59_0235.txt	2	0.128611	0.552889	0.111667	0.188444
Neurotrophil	11				
Eosinophil	1				
Basophil	1				
Lymphocyte	4				
Monocyte	3				

*Figure 69. Counted Cell of YOLOv5l using Image Enhancement Data*

The third trial shows that the three models have the same performance with other models mostly where none of the WBCs is detected from a total of 0 WBCs and only red blood cells were provided. And the last test is to try to detect myelocytes which are undefined subtypes of WBC in this study. There are 5 basophils in 5 images where each image has myelocytes. From the results of calculations performed, the YOLOv5l model generated from the accumulation of

original data and augmented dataset with image enhancement based has the same ability not to identify myelocytes into the model.

*Table 24. Detection and Counting of Built Model with Image Enhancement Augmentation-based for Unidentified Cell in an Image*

No	Class	Correct	YOLOv5s	YOLOv5l	YOLOv5x
0	Neutrophil	0	0	0	0
1	Eosinophil	0	0	0	0
2	Basophil	5	5	5	5
3	Lymphocyte	0	0	0	0
4	Monocyte	0	0	0	0



## CHAPTER 5 CONCLUSION

### 5.1. Conclusion

The identification and counting of subtypes of WBC using Neural Network with limited raw data can be done by means of microscopic observation and model development. This study develops seven models based on three models from the YOLOv5 family with different types of dataset preparation. From the model development process that has been completed, the YOLOv5l model built from the raw dataset is the best model with an accuracy of mAP@.5 0.995 and 0.946 mAP@.5:.95 at 600 epochs of training. From three different datasets, the best model to be applied for detecting and counting subtypes of WBC is YOLOv5l. The best dataset preparation is able to be trained strongly with the accumulation of original dataset and augmented data with image enhancement based. In detecting multiple images, YOLOv5x generally seems remarkable in performing detection.

The detection accuracy of the Convolutional Neural Network is figured out by performing data enrichment through augmentation techniques for identification of subtypes of WBC. The best model of the four models built is YOLOv5l model built from the image enhancement-based dataset is the best model with an accuracy of mAP@.5 0.995 and 0.988 mAP@.5:.95 at 600 epochs of training.

### 5.2. Future Work

To complete this research, there are five points need to be concerned. The first, model development which is supported by data enrichment process through augmentation technique needs to be re-evaluated to avoid underfitting and overfitting. Therefore, the number of datasets, variations and multiplication factors used need to be re-analyzed to get better performance results. Additionally, for the augmentation procedure using image enhancement can be explored more in other techniques.

To perform high performance in real implementation, the second point is to build an application on subtypes of WBC identification based by combining the detection procedure with the real-time mechanism. The third, it is needed to enhance this work by optimizing the speed and performance of the developed work for haematocytes recognition. The next is developing data center for open-source dataset under the ethic review committee is able to be conducted to support the health service performance. And the last is making sustainable team in blood analysis using deep learning is better way to boost the development process to face digital health service.



## REFERENCES



จุฬาลงกรณ์มหาวิทยาลัย  
**CHULALONGKORN UNIVERSITY**

- [1] G. Thiru, "Indonesian health tech startup Halodoc scores \$80M in Series C funding," 2021. [Online]. Available: <https://www.mobihealthnews.com/news/asia/indonesian-health-tech-startup-halodoc-scores-80m-series-c-funding>. [Accessed 10 12 2021].
- [2] A. F. Agung, H. Prabowo, M. Ali, M. G. A. Pradana and S. B. Worsito, "Alat Terapi Otot Dan Sendi Pada Lengan Untuk Penderita Stroke Melalui Smartphone Android". Indonesia Patent IDP000078860, 03 09 2021.
- [3] G. Moreen, "SDG Talks Vol. 12: Telmedicine: The Rise of Telehealth Services During COVID-19," 2020. [Online]. Available: [https://www.id.undp.org/content/indonesia/en/home/presscenter/articles/2020/SDG-Talks-Vol-12.html?utm\\_source=EN&utm\\_medium=GSR&utm\\_](https://www.id.undp.org/content/indonesia/en/home/presscenter/articles/2020/SDG-Talks-Vol-12.html?utm_source=EN&utm_medium=GSR&utm_). [Accessed 20 11 2021].
- [4] M. Sajjad, S. Khan, Z. Jan, H. Moon, J. T. Kwak, S. Rho, S. W. Baik and I. Mehmood, "Leukocytes Classification and Segmentation in Microscopic Blood Smear: A Resource-Aware Healthcare Service in Smart Cities," *IEEE Access*, vol. 5, pp. 3475-3489, 2017.
- [5] "The AI Industry Series: Top Healthcare AI Trends To Watch," CBInsights, 2019. [Online]. Available: <https://www.cbinsights.com/research/report/ai-trends-healthcare/>. [Accessed 11 11 2021].
- [6] K. A. Fahad and H. G. Wael, "Blood Diseases Detection using Classical Machine Learning Algorithms," *International Journal of Advanced Computer Science and Applications(IJACSA)*, vol. 10, no. 7, 2019.
- [7] M. Sam, F. Steve, Y. Frank, D. Stoyan, N.-S. Karin, R. P. William and O. Aydogan, "A Mathematical Framework for Combining Decisions of Multiple

Experts toward Accurate and Remote Diagnosis of Malaria Using Tele-Microscopy," *PLoS One*, 11 October 2012.

- [8] N. Fajarina, "Berkenalan dengan Jenis Leukosit dan Fungsinya, Serta Jumlah Normal dalam Tubuh," 2021. [Online]. Available: <https://hellosehat.com/kelainan-darah/sel-darah-putih/leukosit/>. [Accessed 12 2021].
- [9] Y. Abubakar, I. Faisal, A. Usman and H. T. Syed, "Image processing based detection & classification of blood group using color images," *2017 International Conference on Communication, Computing and Digital Systems (C-CODE)*, pp. 293-298, 2017.
- [10] G. Ravindran, T. J. Titus, M. Pravin and P. Pandiyan, "Determination and Classification of Blood Types using Image Processing Techniques," *International Journal of Computer Applications*, pp. 12-16, 1 1 2017.
- [11] A. S. Ashour, Maram A Wahba and R. Ghannam, "A Cascaded Classification-Segmentation Reversible System for Computer-Aided Detection and Cells Counting in Microscopic Peripheral Blood Smear Basophils and Eosinophils Images," *IEEE Access*, vol. 9, pp. 78883-78901, 2021.
- [12] D. Wang, M. Hwang, W.-C. Jiang, K. Ding, H. C. Chang and K.-S. Hwang, "A deep learning method for counting white blood cells in bone marrow images," *Proceedings of the International Conference on Biomedical Engineering Innovation (ICBEI) 2019-2020*, vol. 22 Supplement 5, 2021.
- [13] S. Igarashia, Y. Sasakib, T. Mikamia, H. Sakurabaa and S. Fukudaa, "Anatomical classification of upper gastrointestinal organs under various image capture conditions using AlexNet," *Computers in Biology and Medicine*, vol. 124, p. 103950, 2020.

- [14] S. Kadry, V. Rajinikanth, D. Taniar, R. Damaševičius and X. P. B. Valencia, "Automated segmentation of leukocyte from hematological images—a study using various CNN schemes," *The Journal of Supercomputing*, 2021.
- [15] M. Sharif, J. Amin, A. Siddiqa, H. U. Khan, M. S. A. Malik, M. A. Anjum and S. K. , "Recognition of Different Types of Leukocytes using YOLOv2 and Optimized Bag-of-Features," *IEEE Access*, 2020.
- [16] Mayo Clinic, "Complete blood count (CBC)," [Online]. Available: <https://www.mayoclinic.org/tests-procedures/complete-blood-count/about/pac-20384919>. [Accessed 10 12 2021].
- [17] K. A. Setiaputri and M. Yosia, "Macam Komponen Darah Manusia dan Fungsinya," 26 7 2021. [Online]. Available: <https://hellosehat.com/kelainan-darah/darah-lainnya/komponen-darah-manusia/>. [Accessed 10 12 2021].
- [18] Cleveland Clinic Medical Professional, "Function of White Blood Cells," 23 7 2021. [Online]. Available: <https://my.clevelandclinic.org/health/body/21871-white-blood-cells>. [Accessed 12 12 2021].
- [19] K. Adrian, "Leukosit Tinggi: Ini Penyebab dan Gejalanya," *Alodokter*, 8 6 2020. [Online]. Available: <https://www.alodokter.com/leukosit-tinggi-ini-penyebab-dan-gejalanya>. [Accessed 10 12 2021].
- [20] IBM, "Machine Learning," 20 7 2020. [Online]. Available: [https://www.ibm.com/cloud/learn/machine-learning#toc-how-machin-NoVMSZI\\_](https://www.ibm.com/cloud/learn/machine-learning#toc-how-machin-NoVMSZI_). [Accessed 11 12 2021].
- [21] Pioneer Labs, "The Three Types of Machine Learning Algorithms," 2020. [Online]. Available: <https://pioneerlabs.io/insights/the-three-types-of-machine-learning-algorithms/>. [Accessed 11 12 2021].

- [22] Develop Paper, "Dawnbench at Stanford: Huawei cloud modelarts in-depth learning and training is the fastest in the world," 22 12 2019. [Online]. Available: <https://developpaper.com/dawnbench-at-stanford-huawei-cloud-modelarts-in-depth-learning-and-training-is-the-fastest-in-the-world/>. [Accessed 20 11 2021].
- [23] J. Deng, W. Dong, R. Socher, L.-J. Li, K. Li and L. Fei-Fei, "ImageNet: A large-scale hierarchical image database," *2009 IEEE Conference on Computer Vision and Pattern Recognition*, pp. 248-255, 2009.
- [24] A. Krizhevsky, I. Sutskever and G. E. H. Hinton, "ImageNet classification with deep convolutional neural networks," in *Proceedings of the 25th International Conference on Neural Information Processing Systems (NIPS '12)*, Lake Tahoe, NV, USA, 3-6 December 2012.
- [25] I. W. S. E. Putra, A. Y. Wijaya and R. Soelaiman, "Klasifikasi Citra Menggunakan Convolutional Neural Network (Cnn) pada Caltech 101," *JURNAL TEKNIK ITS*, vol. 1, no. ISSN: 2337-3539, pp. 2301-9271, 2016.
- [26] R. N. Keiron O'Shea, "An Introduction to Convolutional Neural Networks," *arXiv.org*, no. 1511.08458, 2015.
- [27] R. Girshick, J. Donahue, T. Darrell and J. Malik, "Rich feature hierarchies for accurate object detection and semantic segmentation," *arXiv*, no. 311.2524v5, 22 Oct 2014.
- [28] A. F. Joseph Redmon, "YOLOv3: An Incremental Improvement," *arXiv*, vol. 1804.02767, 8 Apr 2018.
- [29] R. Xu, H. Lin, K. Lu, L. Cao and Y. Liu, "A Forest Fire Detection System Based on Ensemble Learning," *Forests*, no. 217, 2021.

- [30] S. M. Ali, "Comparative Analysis of YOLOv3, YOLOv4 and YOLOv5 for Sign Language Detection," *IJARIE-ISSN(O)*, vol. 7, no. 4, pp. 2395-4396, 2021.
- [31] J. Omony, "Re: Is there an ideal ratio between a training set and validation set? Which trade-off would you suggest? Retrieved from:," *Research Gate*, 2021.
- [32] Ultralytics, "Tips for Best Training Results.," 2019.
- [33] V. K. O. K. Afshin Gholamy, "Why 70/30 or 80/20 Relation Between Training and Testing Sets: A Pedagogical Explanation," *Technical Report: UTEP-CS-18-09*, 2018.
- [34] M. T. I. A. F. A. Amran Hossain, "A Deep Learning Model to Classify and Detect Brain Abnormalities in Portable Microwave Based Imaging System," *Research Square*, 30 August 2021.
- [35] Z. Liu, X. Jia and X. Xu, "Study of shrimp recognition methods using smart networks," *Computers and Electronics in Agriculture*, vol. 165, no. 104926, 2019.
- [36] P. C. N. W. W. P. S. P. Natthakorn Kasamsumran, "Applying Faster R-CNN for Hematocytes Detection on Compound Microscope with Image Sensor Device and Multiple GPU Computation," *2020 8th International Electrical Engineering Congress (iEECON)*, pp. 1-4, 2020.
- [37] S. A. Singh, How much data-set sample is enough for classification using training and validation based on deep learning approach like AlexNet or GoogleNet?, [https://www.researchgate.net/post/How\\_much\\_data-set\\_sample\\_is\\_enough\\_for\\_classification\\_using\\_training\\_and\\_validation\\_based\\_on\\_deep\\_learning\\_approach\\_like\\_AlexNet\\_or\\_GoogleNet](https://www.researchgate.net/post/How_much_data-set_sample_is_enough_for_classification_using_training_and_validation_based_on_deep_learning_approach_like_AlexNet_or_GoogleNet), 2019.



- [38] L. G. Arie, The practical guide for Object Detection with YOLOv5 algorithm, <https://towardsdatascience.com/the-practical-guide-for-object-detection-with-yolov5-algorithm-74c04aac4843>, 2022.



## VITA

<b>NAME</b>	Singgih Bekti Worsito
<b>DATE OF BIRTH</b>	03 August 1996
<b>PLACE OF BIRTH</b>	Grobogan
<b>INSTITUTIONS ATTENDED</b>	Yogyakarta State University
<b>HOME ADDRESS</b>	Ds. Sugihan RT 001 RW 007, Kecamatan Toroh, Kabupaten Grobogan, Provinsi Jawa Tengah, Indonesia
<b>PUBLICATION</b>	- Image-Based White Blood Cell Subtype Detection Using ResNet-50 Convolutional Neural Network (CNN)
<b>AWARD RECEIVED</b>	<ul style="list-style-type: none"><li>- Certified in Front End Developer (HTML, CSS, JavaScript) by Progate in 2022</li><li>- Certified in Programmer by Lembaga Sertifikasi Profesi (LSP) Indonesia in 2021</li><li>- A Grade on AI for Future Workforce in 2021</li><li>- Participant in Python Programming for Video Analytics Training Worksop in 2022</li><li>- Selected Team in Circular Innovation Challenge 2022</li><li>- Student Exchange "Working in Multicultural Teams" held by Tokyo Institute of Technology in 2022</li><li>- ASEAN Data Science Explorer 2021 Enablement Session – held by SAP and ASEAN Foundations in 2021</li><li>- 2021 Local Knowledge Acquisition Program Award Certificate - given by The National Research and Innovation Agency (BRIN) of Indonesia</li><li>- Training on AI with a Cause with HUAWEI in 2021</li><li>- Speaker at Policy Talk – held by Directorate of Study and Research of Overseas Indonesian Students' Association Alliance (OISAA / PPI Dunia) in 2021</li></ul>

- Training Certificate of How to Install Rooftop Solar PV from A to Z in 2021

- Staff in the RoboCup Small Size League (SSL) Competition, Bangkok, Thailand in 2022

- Presenter in 2021 International Conference on Instrumentation, Control, and Automation (ICA)

- Presenter in The 14th Regional Conference on Electrical and Electronics Engineering (RC-EEE 2021), Bangkok, Thailand

- Organizing Committee of AASIC - ASIAN Academic Society International Conference - an annual event conducted by PERMITHA (Overseas Indonesia Student Association in Thailand) and Embassy of The Republic of Indonesia (KBRI) for The Kingdom of Thailand, Education and Culture Attache in 2021